Noncatalytic Bruton's tyrosine kinase activates PLCγ_2 variants mediating ibrutinib resistance in human chronic lymphocytic leukemia cells

Received for publication, November 18, 2019, and in revised form, February 26, 2020 Published, Papers in Press, March 17, 2020, DOI 10.1074/jbc.RA119.011946

Martin Wist[‡], Laura Meier[‡], Orit Gutman[§], Jennifer Haas[‡], Sascha Endres[‡], Yuan Zhou[‡], Reinhild Rösler[¶], Sebastian Wiese[¶], Stephan Stilgenbauer[‖], Elias Hobeika[**], Yoav I. Henis[§1], Peter Gierschik[‡2], and Claudia Walliser[‡3]

From the [‡]Institute of Pharmacology and Toxicology, Ulm University Medical Center, 89081 Ulm, Germany, the [§]Department of Neurobiology, George S. Wise Faculty of Life Sciences, Tel Aviv University, Tel Aviv 69978, Israel, the [¶]Core Unit Mass Spectrometry and Proteomics, Medical Faculty, Ulm University Medical Center, 89081 Ulm, Germany, the [‖]Department of Internal Medicine III, Ulm University Medical Center, 89081 Ulm, Germany, and the [**]Institute of Immunology, Ulm University Medical Center, 89081 Ulm, Germany

Edited by Alex Toker

Treatment of patients with chronic lymphocytic leukemia (CLL) with inhibitors of Bruton's tyrosine kinase (BTK), such as ibrutinib, is limited by primary or secondary resistance to this drug. Examinations of CLL patients with late relapses while on ibrutinib, which inhibits BTK's catalytic activity, revealed several mutations in *BTK*, most frequently resulting in the C481S substitution, and disclosed many mutations in *PLCG2*, encoding phospholipase C-γ_2 (PLCγ_2). The PLCγ_2 variants typically do not exhibit constitutive activity in cell-free systems, leading to the suggestion that in intact cells they are hypersensitive to Rac family small GTPases or to the upstream kinases spleen-associated tyrosine kinase (SYK) and Lck/Yes-related novel tyrosine kinase (LYN). The sensitivity of the PLCγ_2 variants to BTK itself has remained unknown. Here, using genetically-modified DT40 B lymphocytes, along with various biochemical assays, including analysis of PLCγ_2-mediated inositol phosphate formation, inositol phospholipid assessments, fluorescence recovery after photobleaching (FRAP) static laser microscopy, and determination of intracellular calcium ($[Ca^{2+}]_i$), we show that various CLL-specific PLCγ_2 variants such as PLCγ_2S707Y are hyperresponsive to activated BTK, even in the absence of BTK's catalytic activity and independently of enhanced PLCγ_2 phospholipid substrate supply. At high levels of B-cell receptor (BCR) activation, which may occur in individual CLL patients, catalytically-inactive BTK restored the ability of the BCR to mediate increases in $[Ca^{2+}]_i$. Because catalytically-inactive BTK is insensitive to active-site BTK inhibitors, the mechanism involving the noncatalytic BTK uncovered here may contribute to preexisting reduced sensitivity or even primary resistance of CLL to these drugs.

The two members of the γ subfamily of inositol phospholipid–specific phospholipase C (PLC),[4] PLCγ_1 and PLCγ_2, have recently been found to be involved in a number of ostensibly different human disease states (1). These range from rare hereditary diseases caused by, or associated with, germline mutations in the *PLCG2* gene, such as complex immunological diseases with an autoinflammatory hallmark (2, 3) and childhood-onset steroid-sensitive nephrotic syndrome (4), to acquired conditions associated with somatic *PLCG1* or *PLCG2* mutations, such as angiosarcoma and T-cell lymphomas (*PLCG1*) (5, 6), and endemic Burkitt lymphoma (*PLCG2*) (7). Point mutations in *PLCG2* have also been reported to modify the risk of developing neurodegenerative diseases like Alzheimer's disease (8, 9) and to cause resistance of chronic lymphocytic leukemia (CLL) cells to catalytic-site inhibitors of Bruton's tyrosine kinase (BTK) (10).

BTK is one of the five members of the strongly-conserved Tec family of nonreceptor tyrosine kinases, also including the IL-2–inducible T-cell kinase ITK, TEC proper, RLK, and BMX (11). Although all five Tec variants are expressed in cells of the hematopoietic lineage, BTK and ITK are key regulators of B-cell and T-cell transmembrane signaling, respectively (12). Mutations of the human and mouse *BTK* and *Btk* genes functionally affecting BTK were found to be associated with human

This work was supported by Deutsche Forschungsgemeinschaft (DFG) Grants SFB 1074/TP A8 and GSC 279 and the Ministerium für Wissenschaft, Forschung, und Kunst Baden-Württemberg (PharmCompNet BW). The authors declare that they have no conflicts of interest with the contents of this article.

This article contains Figs. S1–S6 and Table S1.

[1] Holds the Zalman Weinberg Chair in Cell Biology.

[2] To whom correspondence may be addressed: Institute of Pharmacology and Toxicology, University of Ulm Medical Center, Albert-Einstein-Allee 11, 89081 Ulm, Germany. Tel.: 49-731-5006 5500; Fax: 49-731-5006 5502; E-mail: peter.gierschik@uni-ulm.de.

[3] To whom correspondence may be addressed: Institute of Pharmacology and Toxicology, University of Ulm Medical Center, Albert-Einstein-Allee 11, 89081 Ulm, Germany. Tel.: 49-731-5006 5500; Fax: 49-731-5006 5502; E-mail: claudia.walliser@uni-ulm.de.

[4] The abbreviations used are: PLC, inositol phospholipid-specific phospholipase C; RAC, Ras-related C3 botulinum toxin substrate; BTK, Bruton's tyrosine kinase; PIP5K, phosphatidylinositol-4-phosphate 5-kinase; BCR, B-cell receptor; $[Ca^{2+}]_i$, intracellular calcium ion concentration; PtdInsP_3, phosphatidylinositol 3,4,5-trisphosphate; PtdInsP_2, phosphatidylinositol 4,5-bisphosphate; CLL, chronic lymphocytic leukemia; WM, Waldenström's macroglobulinemia; FRAP, fluorescence recovery after photobleaching; NFAT, Ca^{2+}-regulated nuclear factor of activated T cells; XLA, human X-linked agammaglobulinemia; ANOVA, analysis of variance; CFSE, 5-(and-6)-carboxyfluorescein diacetate succinimidyl ester; SH, Src homology; PH, pleckstrin homology; v-SRC, rous sarcoma virus tyrosine kinase.

X-linked agammaglobulinemia (XLA) and murine X-linked immunodeficiency (11). BTK and the other Tec family members share an overall similar domain organization that closely resembles the organization of the Src family tyrosine kinases, with an SH3–SH2–protein-tyrosine kinase domain tandem at their C termini, but divergent N-terminal regions (11). In B cells, BTK couples antigen-activated B-cell receptors (BCR) to tyrosine phosphorylation of PLCγ_2 at the four canonical tyrosine residues, Tyr-753, Tyr-759, Tyr-1197, and Tyr-1217 (13, 14). The latter modifications activate PLCγ_2 to hydrolyze its substrate phosphatidylinositol 4,5-bisphosphate (PtdInsP_2) to inositol 1,4,5-trisphosphate and diacylglycerol. All three of the latter act as intracellular second messengers (15, 16), which are involved in controlling key functions of both normal and neoplastic B lymphocytes. The activation of PLCγ_2 is greatly facilitated by the adaptor protein BLNK/SLP-65 (17, 18) and requires membrane targeting of BTK via its N-terminal pleckstrin homology domain to phosphatidylinositol 3,4,5-trisphosphate generated from PtdInsP_2 by phosphatidylinositol 3-kinases. For this reason, it can be blocked by the R28C and mimicked by the E41K mutation within its PH domain (19, 20). The K430R mutation of BTK, by replacing a crucial lysine coordinating the α- and β-phosphates of the substrate ATP and being present in this position in all protein kinases (21), renders the BTK protein catalytically inert (22).

Previous experimentation has shown that, during B-cell development, BTK partially acts as an adaptor molecule, independent of its catalytic activity (23), and that the tumor suppressor function of BTK identified in pre-B cells is independent of its catalytic activity (24). Specifically, kinase-inactive BTKK430R completely reconstituted λ usage in BTK-deficient mice and partially corrected the defective modulation of pre-B cell–surface markers, peripheral B-cell survival, and BCR-mediated NF-κB induction (23). Activation of BTK by pre-BCR stimulation was also shown to be independent of BLNK/SLP-65 (24). These effects have thus far been attributed to the observation that BTK associates with phosphatidylinositol-4-phosphate 5-kinases (PIP5Ks), the enzymes that synthesize the generic substrate of inositol phospholipid–specific phospholipase C, PtdInsP_2 (25).

Irreversible BTK inhibitors such as ibrutinib have demonstrated remarkable activity in a number of B-cell malignancies with approval in CLL, mantle cell lymphoma, marginal zone lymphoma, and Waldenström's macroglobulinemia (26, 27). As a result, ibrutinib is being used with increasing frequency as frontline therapy, beginning to displace chemoimmunotherapy in this setting (28, 29). Currently, the drugs are also being evaluated for the treatment of other diseases, such as other malignancies and various autoimmune and/or inflammatory diseases (30–33). As is the case for other targeted tumor therapies, BTK inhibitor treatment of CLL is limited by either primary or secondary, *i.e.* acquired drug resistance (10). Thus, whole-exome sequencing of CLL cells causing late relapses revealed (i) C481S and a small number of other mutations in the same and in other positions in *BTK* and (ii) a higher variety of mutations in *PLCG2.* To date, some 25 point mutations of one or two adjacent residues are known in *PLCG2*, some of which cluster in specific regions of the encoded PLCγ_2 protein, such as one of the two SH2 domains and the C2 domain (34–36). Collectively, the *BTK* and *PLCG2* mutations are associated with about 85% of CLL cases with acquired resistance to BTK inhibitors (37).

Although the C481S mutation of *BTK* eliminates covalent binding of some BTK inhibitors, such as ibrutinib, to their target and hence markedly reduces their affinity to their binding site, the mechanism of resistance caused by the other *BTK* and the *PLCG2* mutations is less clear. PLCγ_2 is immediately downstream of BTK (26) leading to the suggestion that the variant proteins may be constitutively active. However, we have previously found that several PLCγ_2 variant enzymes associated with ibrutinib resistance carrying mutations in various regions are not constitutively active when assayed, even as purified proteins, in a cell-free system employing artificial lipid vesicles as substrate (38, 39). The observation that PLCγ_2 variants are, instead, hypersensitive in intact cells to the Rho GTPase RAC2, as well as the upstream protein-tyrosine kinases SYK and LYN (39, 40), has led us to suggest that the *PLCG2* mutations found in BTK inhibitor–resistant cells may cause a rerouting of the transmembrane signals emanating from BCR to converge on and activate PLCγ_2.

This work was undertaken to study the functional interaction of BTK with PLCγ_2, WT, and ibrutinib resistance variants in a system reconstituted in intact cells from the two protein constituents. We chose enhanced inositol phosphate formation as a functional readout of a productive interaction between the two, rather than PLCγ_2 phosphorylation, as it is the most relevant functional outcome of stimulated PLCγ_2 in terms of B-cell signaling. Also PLCγ_2 is phosphorylated at many other residues, for instance Tyr-733 or Tyr-1245, in addition to the four canonical sites utilized by activated BTK (41, 42), which may confound results. To our knowledge, this approach has not been reported previously. Here, we report that several PLCγ_2 variants mediating BTK-inhibitor resistance in CLL patients are strikingly hypersensitive to activated and/or membrane-bound BTK and to BTK variants lacking protein-tyrosine kinase activity. Importantly, we demonstrate that the activity of the PLCγ_2 variants in the context of catalytically-inactive BTK is not contingent on enhanced formation of the PLC substrate PtdInsP_2 via stimulation of PtdIns*P* kinases, as postulated earlier. Hence, stimulation of PLCγ_2 variants mediating BTK inhibitor resistance can be explained by their hypersensitivity to the noncatalytic actions of BTK. We suggest that this mechanism contributes to the acquired BTK inhibitor resistance observed in CLL patients with *PLCG2* mutations and, potentially, to preexisting reduced sensitivity or even primary resistance of clonal populations of CLL cells with hyperactivated BCR.

Results

PLCγ_2S707Y can be functionally reconstituted with and is hypersensitive to activation by BTK

To investigate and compare the functional reconstitution of various PLC isozymes with WT BTK and its predominantly membrane-bound and, hence, active variant E41K, WT PLCγ_1, PLCγ_2, PLCβ_2, WT, and Δ44 variant PLCδ_1, and S707Y variant PLCγ_2 were coexpressed with the two BTK variants in COS-7

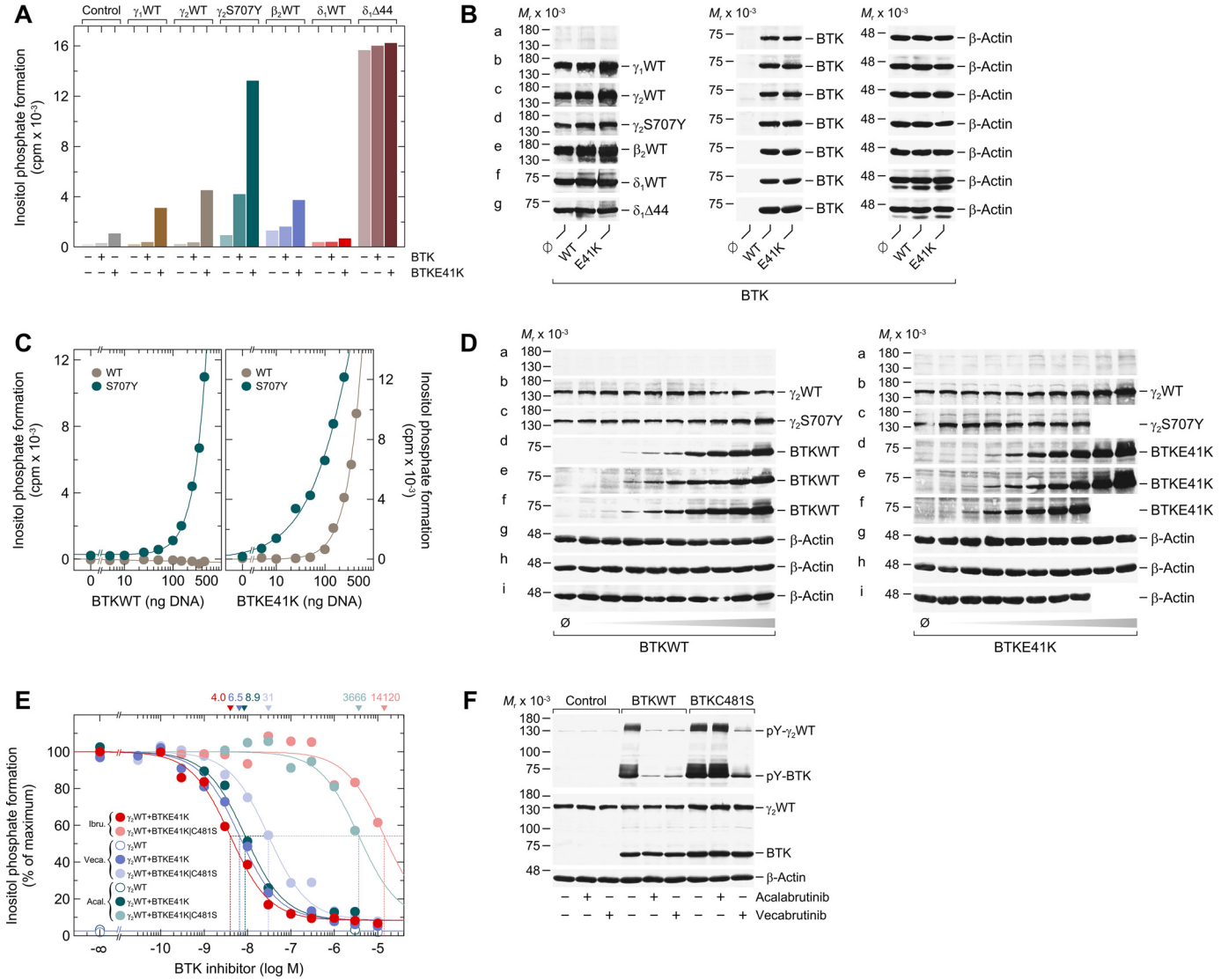

Figure 1. Analysis of the functional reconstitution of PLCγ_2 and BTK. *A,* COS-7 cells were transfected as indicated with 250 ng/well of either empty vector (*Control*) or 150 ng/well of vector encoding either WT PLCγ_1 (*γ_1WT*), WT PLCγ_2 (*γ_2WT*), WT PLCβ_2 (*β_2WT*), or WT PLCδ_1 (*δ_1WT*), 50 ng/well of vector encoding PLCγ_2S707Y (*γ_2S707Y*) or PLC$\delta_1\Delta44$ (*$\delta_1\Delta44$*), and 100 ng/well of vector encoding either WT BTK (*BTKWT*) or a constitutively-active version of BTK (*BTKE41K*). *B,* cells from one well each functionally analyzed in *A* were washed with 0.2 ml of Dulbecco's PBS and then lysed by addition of 100 μl of SDS-PAGE sample preparation buffer. Aliquots of the samples were subjected to SDS-PAGE, and immunoblotting was performed using an antibody reactive against the c-Myc epitope present on WT PLCγ_1, WT PLCγ_2, PLCγ_2S707Y, WT PLCδ_1, and PLC$\delta_1\Delta44$ (*a–d* and *f–g*), antibody reactive against PLCβ_2 (*e*), antibody reactive against BTK (*a–g*), or antibody reactive against β-actin (*a–g*). *C,* COS-7 cells were transfected as indicated with 50 ng/well of vector encoding WT PLCγ_2 (*γ_2WT*) or PLCγ_2S707Y (*γ_2S707Y*) and increasing amounts (0–450 ng/well) of vector encoding WT BTK (*BTKWT*) (*left panel*) or BTKE41K (*right panel*). *A* and *C,* 24 h after transfection, the cells were incubated for 18 h with *myo*-[2-^{3}H]inositol, and inositol phosphate formation was then determined. *D,* cells from one well each functionally analyzed in *C* were washed with 0.2 ml of Dulbecco's PBS and then lysed by addition of 100 μl of SDS-PAGE sample preparation buffer. Aliquots of the samples were subjected to SDS-PAGE, and immunoblotting was performed using an antibody reactive against the c-Myc epitope present on WT PLCγ_2 and PLCγ_2S707Y (*a–c*), antibody reactive against BTK (*d–f*), or antibody reactive against β-actin (*g–i*). *E,* COS-7 cells were transfected as indicated with 150 ng/well of vector encoding WT PLCγ_2 (*γ_2WT*) and 100 ng/well of vector encoding BTKE41K or BTKE41K/C481S. Twenty four hours after transfection, the cells were incubated for 18 h with *myo*-[2-^{3}H]inositol and either solvent (0.1% (v/v) DMSO) or increasing amounts of ibrutinib (0.1 nM to 10 μM), vecabrutinib (0.1 nM to 10 μM), or acalabrutinib (1 nM to 3 μM). Inositol phosphate formation was then determined. The results were normalized to percent of maximal inositol phosphate formation, which was 10,012, 9747, and 15,178 cpm for ibrutinib, acalabrutinib, and vecabrutinib, respectively. The IC_{50} values of ibrutinib, acalabrutinib, and vecabrutinib for the inhibition of BTKE41K and BTKE41K/C481S obtained by nonlinear curve fitting are shown above the graph in nM. *F,* COS-7 cells were transfected as indicated with 1.33 μg/well of vector encoding WT PLCγ_2 (*γ_2WT*) and 0.66 μg/well of empty vector (*Control*) or vector encoding BTKWT or BTKC481S. Twenty four hours after transfection, the cells were incubated for 18 h, as indicated with either solvent (0.1% (v/v) DMSO), acalabrutinib (1 μM), or vecabrutinib (1 μM). Cells were lysed, and immunoblotting was performed as indicated using an antibody reactive against the c-Myc epitope present on WT PLCγ_2, antibody reactive against BTK, antibody reactive against β-actin, antibody reactive against phosphorylated tyrosine on PLCγ_2 at position 759 (*pY-PLCγ_2*), and antibody reactive against phosphorylated tyrosine on BTK at position 223 (*pY-BTK*). *A*, *C*, *E*, and *F* show representative results from three independent experiments each as mean values of three technical replicates.

cells radiolabeled with [^{3}H]inositol for measurement of [^{3}H]inositol phosphate formation (Fig. 1*A*). WT and constitutively-active Δ44 variants of the evolutionarily divergent PLC isoform PLCδ_1, carrying a deletion of the autoinhibitory *X-Y* linker (43), were analyzed for comparison. PLCδ_1 is not known to be regulated by heterotrimeric GTP-binding proteins or members of the Tec kinase family and is thus considered to be distinct from a mechanistic point of view. There was little effect

of WT BTK on inositol phosphate formation in the absence of exogenous PLC enzymes and in the presence of any of the WT PLCs. In contrast, in the presence of PLCγ_2S707Y, WT BTK caused a 4.6-fold increase in inositol phosphate formation. BTKE41K caused a minor increase in inositol phosphate formation in the absence of exogenous PLCs but triggered much more marked increases in the presence of WT PLCγ_1, PLCγ_2, PLCβ_2, and, most strikingly, of PLCγ_2S707Y. Neither WT nor Δ44 variant PLCδ_1 activity was affected by WT or E41K variant BTK, suggesting that the stimulatory effects observed for the other PLC isozymes were not due to enhanced supply of their common substrate PtdInsP_2. Fig. 1*B* shows that the differences in inositol phosphate formation observed in Fig. 1*A* were not explained by differences in protein expression. Note that there was no difference in the expression of WT PLCγ_2 and PLCγ_2S707Y when directly compared on the same immunoblots (*cf.* Fig. 3*D* and Fig. S3).

Fig. 1*C* shows the dependence of WT *versus* S707Y variant PLCγ_2 activity on increasing expression levels of WT *versus* E41K variant BTK after correction of inositol phosphate formation for background activity observed in the absence of exogenous PLCγ enzyme. In contrast to WT PLCγ_2 activity, which was unaffected by WT BTK even at the highest expression level, PLCγ_2S707Y variant activity was markedly stimulated by WT BTK in a concentration-dependent fashion. Furthermore, increased expression of BTKE41K caused striking increases in the activities of both WT and S707Y variant PLCγ_2, although the variant was severalfold more sensitive to BTKE41K. The E41K mutation also rendered BTK more potent in activating PLCγ_2S707Y (*cf.* Fig. 1*C, left versus right panel*). There were no differences in protein expression that would explain the functional differences shown in Fig. 1*C* (*cf.* Fig. 1*D*).

To determine whether the productive interaction between WT PLCγ_2 and BTKE41K (Fig. 1*C*, *right panel*) was contingent on the protein-tyrosine kinase activity of BTKE41K, the effects of BTK protein-tyrosine kinase inhibitors, ibrutinib, acalabrutinib, and vecabrutinib, were investigated (Fig. 1*E*). In addition, the effect of the *BTK* C481S mutation was tested by incorporating this mutation into a BTKE41K/C481S compound variant. The C481S mutation is known to cause resistance to the two irreversible covalent BTK inhibitors, ibrutinib and acalabrutib, with limited, if any, impact on vecabrutinib activity, a novel noncovalent and reversible BTK inhibitor (44). Fig. 1*E* shows that both the E41K single and the E41K/C481S double variants caused a similar ~38-fold increase in PLCγ_2 activity. All three drugs showed potent inhibition of PLCγ_2 activity in the E41K single variant cells. However, ibrutinib and acalabrutinib reduced inositol phosphate formation by only 50% in PLCγ_2 and BTKE41K/C481S cells. Estimated IC_{50} values of these covalent inhibitors were ~3530-fold (ibrutinib) and 410-fold (acalabrutinib) higher in cells expressing the *BTK* C481S acquired resistance mutation than in cells without this mutation. In contrast, this difference was only about 4.8-fold for vecabrutinib, which does not require BTK Cys-481 interaction for activity. We also tested the effects of acalabrutinib and vecabrutinib at a single concentration, 1 μM, on protein tyrosine phosphorylation of WT PLCγ_2 and either WT BTK or its C481S variant. Fig. 1*F* shows that acalabrutinib was capable of substantially reducing both the autophosphorylation of WT BTK and the BTK-mediated phosphorylation of PLCγ_2, but not of BTKC481S and PLCγ_2, respectively, whereas vecabrutinib was strongly inhibitory in the presence of either WT or C481S variant BTK together with PLCγ_2. Collectively, the results shown in Fig. 1, *E* and *F,* clearly support the view that activation of WT PLCγ_2 by BTKE41K in the reconstituted systems requires the tyrosine kinase activity of BTK.

PLCγ_2S707Y is stimulated by catalytically-inactive BTK independently of tyrosine phosphorylation and increased PtdInsP_2 substrate supply

To interrogate the pharmacology of the BTK-mediated activation of WT and S707Y variant PLCγ_2, both PLCγ_2 variants were coexpressed with WT or variant BTK to examine the effects of 1 μM acalabrutinib on inositol phosphate formation (Fig. 2*A*). Acalabrutinib caused an almost complete loss of the PLCγ_2 activity in BTKE41K cells but, as expected, had a much lower impact in BTKE41K/C481S cells. Surprisingly, acalabrutinib was much less effective in the context of PLCγ_2S707Y-expressing BTKE41K cells, showing only ~25% inhibition. Acalabrutinib had no activity at all in the PLCγ_2S707Y-BTKE41K/C481S cells. Several point variants of BTK were coexpressed with PLCγ_2S707Y to further investigate the functional differences between WT and S707Y variant PLCγ_2 shown in Fig. 2*A* and to also extend this analysis to WT PLCγ_1 (Fig. 2*B*). Point mutations of BTK, Y223F, or Y551F, which prevent tyrosine phosphorylation of BTK in *cis* or in *trans* by upstream protein kinases, and the covalent inhibitor binding site mutation C481S had only small, if any, effects on the ability of WT BTK to mediate PLCγ_2S707Y activation. As expected, modulating the plasma membrane interaction through either inhibitory (R28C) or stimulatory (E41K) mutations caused considerable decreases and increases, respectively, in the reconstitutive activity of BTK. For both WT PLCγ_1 and PLCγ_2, enzyme activation was only observed for the E41K variant of BTK. Most interestingly, however, when BTK protein-tyrosine kinase activity was blocked by the K430R mutation, the BTK-mediated stimulation of PLCγ_2S707Y was only reduced by ~50%. This result, together with those shown in Fig. 2*A*, *right panel*, raised the distinct possibility that PLCγ_2S707Y is sensitive to activation by BTK even in the absence of its tyrosine kinase activity.

To further challenge this hypothesis, WT and S707Y variant PLCγ_2 were coexpressed with increasing concentrations of BTKK430R and its membrane-targeted variant BTKE41K/K430R (Fig. 2*C*, *left panel*). Although the activity of WT PLCγ_2 remained unaffected by the two BTK variants, inositol phosphate formation of the S707Y variant was markedly and concentration-dependently increased. Membrane targeting of even the catalytically incompetent BTK caused an almost 10-fold shift to the left of the concentration–response relationship. The functional effects observed in Fig. 2*C* were unrelated to changes in PLCγ_2 expression (Fig. 2*D*). Analysis of protein tyrosine phosphorylation showed that the two BTK variants, K430R and E41K/K430R, similar to their catalytically-competent counterparts, WT and E41K, in the presence of ibrutinib or acalabrutinib were unable to mediate phosphorylation of the PLCγ_2 residues Tyr-759 or Tyr-1217, *i.e.* known BTK phosphor-

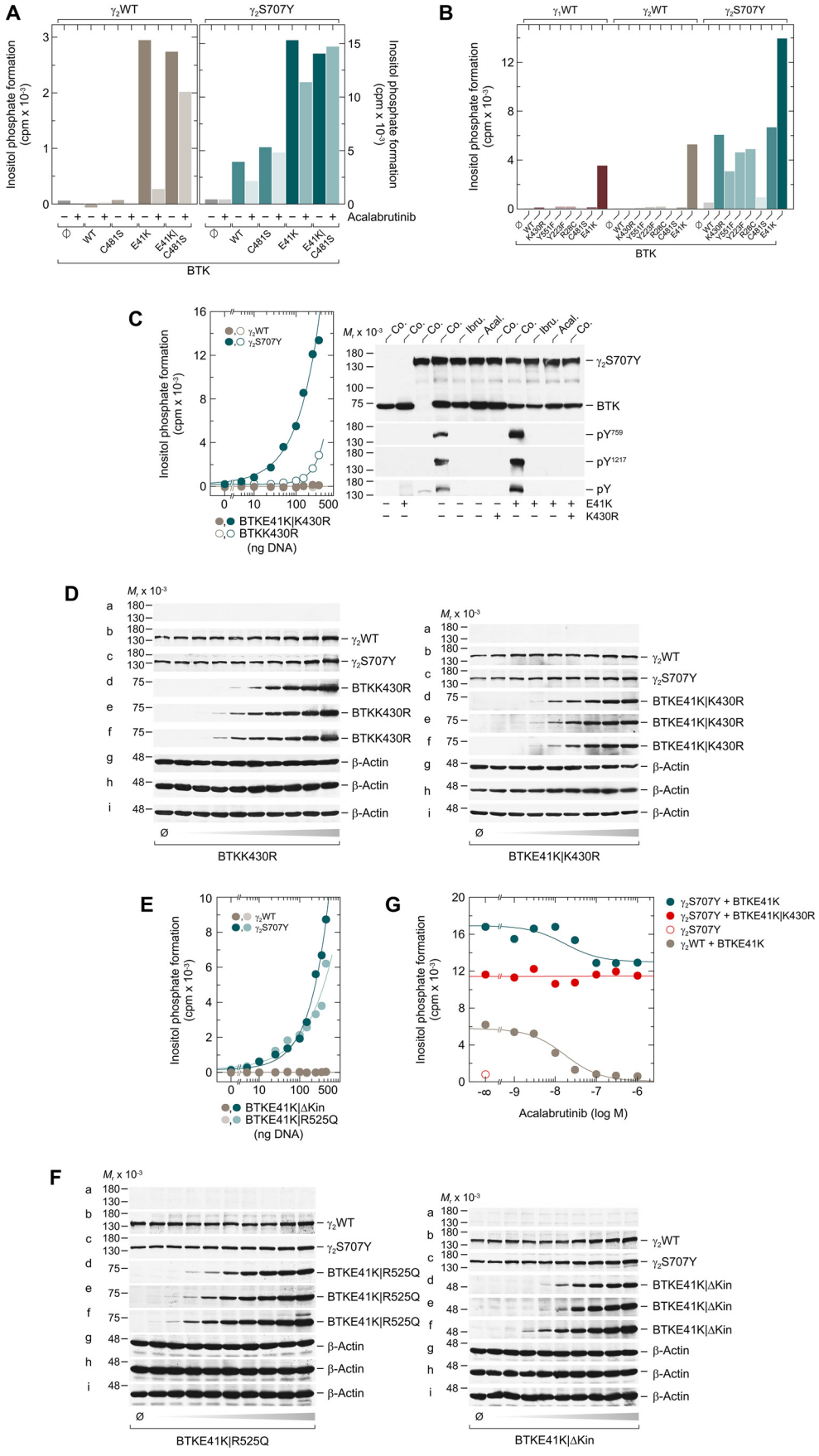
A
γ_2WT
γ_2S707Y
Inositol phosphate formation (cpm x 10^{-3})
Acalabrutinib
BTK
B
γ_1WT
γ_2WT
γ_2S707Y
C
BTKE41K|K430R
BTKK430R
(ng DNA)
pY759
pY1217
pY
E41K
K430R
D
BTKK430R
BTKE41K|K430R
β-Actin
E
BTKE41K|ΔKin
BTKE41K|R525Q
F
BTKE41K|R525Q
BTKE41K|ΔKin
G
γ_2S707Y + BTKE41K
γ_2S707Y + BTKE41K|K430R
γ_2WT + BTKE41K
Acalabrutinib (log M)

ylation sites, or other PLCγ$_2$ tyrosine residues (Fig. 2*C*, *right panel,* subpanels labeled *pY759* and *pY1217*, and *pY*, respectively). Importantly, stimulation of PLCγ$_2$S707Y, but not WT PLCγ$_2$, was not confined to the catalytically-inactive variant K430R and was also observed for another variant devoid of catalytic activity, R525Q (13). This stimulation was even seen for a BTK deletion variant (Δ amino acids 402–659) lacking the protein-tyrosine kinase domain (Fig. 2*E*). Fig. 2*F* shows that the effects of BTK variants on WT and variant PLCγ$_2$ activity observed in Fig. 2*E* were not explained by differences in protein expression. We then determined how the differential sensitivity of the variant PLCγ$_2$S707Y to the actions of both the catalytic and the noncatalytic functions of BTK translates into the concentration dependence of acalabrutinib-mediated BTK inhibition. It is clear from these results that the inhibitor did not affect the strikingly enhanced inositol phosphate formation in the presence of BTKE41K/K430R and PLCγ$_2$S707Y (Fig. 2*G*). Furthermore, acalabrutinib reduced the activities of the BTKE41K/WT PLCγ$_2$ and BTKE41K/PLCγ$_2$S707Y pairs with very similar, if not identical, IC$_{50}$ values (~20 nM), but did so in a markedly different extent. Although enhanced activity was almost fully abrogated in the presence of WT PLCγ$_2$, it was only partially reduced (~23%) in the presence of PLCγ$_2$S707Y, most interestingly to a level very similar to the one observed for catalytically-incompetent BTKE41K/K430R and PLCγ$_2$S707Y. Notably, this level of activity, which was unaffected by acalabrutinib over the whole range of concentrations, was still ~14-fold higher than that observed in the presence of PLCγ$_2$S707Y alone. Therefore, the acalabrutinib resistance of the BTKE41K/PLCγ$_2$S707Y pair is very likely based on the BTK variant exerting tyrosine phosphorylation–independent, stimulatory effects on PLCγ$_2$S707Y.

To address the possibility that the stimulatory effect of membrane-targeted, catalytically-inert BTKE41K/K430R on inositol phosphate formation by PLCγ$_2$S707Y is due to enhanced supply of the enzyme phospholipid substrate directly, the effects of WT as well as E41K, K430R, and E41K/K430R variant BTK on the abundance of the inositol phospholipids, PtdIns, PtdIns*P*, and PtdIns*P*$_2$, in COS-7 cells were examined (Fig. 3*A*). No effect of any of the BTK variants on the abundance of these phospholipids was observed. To further examine potential effects of BTK on substrate availability rather than enzyme activity of PLCγ$_2$, a close congener of PLCγ$_2$S707Y, PLCγ$_1$S729Y, which shares enhanced activity in intact cells with its PLCγ$_2$ counterpart (Fig. 3*B*), was coexpressed with WT as well as variant BTK and functionally compared with PLCγ$_2$S707Y. As shown in Fig. 3*C*, there was a marked difference between the two PLCγ$_2$ variants *vis à vis* BTK, in that PLCγ$_1$S729Y largely behaved like WT PLCγ$_1$ and PLCγ$_2$ and displayed a functional phenotype very different from that of PLCγ$_2$S707Y, which was not due to differences in protein expression (Fig. 3*D*). These results are difficult, if not impossible, to explain by an effect of BTK on substrate availability to the two PLCγ variants in the reconstituted system. Interestingly, the PLCγ$_2$-specific functional phenotype is not restricted to the S707Y variant. Instead, it is also observed for many of the PLCγ$_2$ variants that have previously been associated with ibrutinib resistance of CLL cells: D334H (catalytic subdomain X), R665W, S707F, and S707P (all C-terminal SH2 domain), L845F (C-terminal half of split PH domain), D993H (catalytic subdomain Y), and M1141R (C2 domain) (34, 45, 46). All listed variants were found to be sensitive to stimulation by catalytically-inert BTK (activity ratios BTKE41K/K430R: BTKE41K ≥43.5%; Table 1). Notably, the highest activity ratios, maximal sensitivities for catalytically-inactive BTK, with no difference between BTKE41K and BTKE41K/K430R were observed for the PLCγ$_2$ variants L845F and M1141R. Note that there are no differences in variant PLCγ$_2$ protein expression in the presence of BTKE41K or BTKE41K/K430R. Therefore, the differences in activity ratios BTKE41K/K430R:BTKE41K analyzed for each row of data sets cannot be explained by differences in PLCγ$_2$ and/or BTK protein expression (Fig. S4).

Functional phenotype of PLCγ$_2$S707Y vis à vis BTK is instigated by mutational preactivation of PLCγ$_2$

To determine whether the enhanced sensitivity of PLCγ$_2$S707Y to catalytically-inert BTK is related to its augmented basal activity in intact cells, PLCγ$_2$S707Y was compared with two other variants of PLCγ$_2$ also showing this property, the phosphomimetic variant PLCγ$_2$4E, carrying glutamic acid residues in all four canonical positions of BTK-mediated tyrosine phos-

Figure 2. In contrast to the WT enzyme, the PLCγ$_2$S707Y variant is activated by catalytically-inert BTK. *A,* COS-7 cells were transfected as indicated with 50 ng/well of vector encoding WT PLCγ$_2$ (*γ$_2$WT*) (*left panel*) or PLCγ$_2$S707Y (*γ$_2$S707Y*) (*right panel*) and 150 ng/well of empty vector (*ϕ*) or vector encoding WT BTK (*WT*) or the BTK variants C481S, E41K, or E41K/C481S. Twenty four hours after transfection, the cells were incubated for 18 h with *myo*-[2-^{3}H]inositol and either solvent (0.1% (v/v) DMSO) (−) or 1 μM acalabrutinib (+) prior to determination of inositol phosphate formation. *B,* COS-7 cells were transfected as indicated with 50 ng/well of vector encoding WT PLCγ$_1$ (*γ$_1$WT*), WT PLCγ$_2$ (*γ$_2$WT*), or PLCγ$_2$S707Y (*γ$_2$S707Y*) and 150 ng/well of vector encoding WT BTK (*WT*) or the BTK variants K430R, Y551F, Y223F, R28C, C481S, or E41K. *C, left panel*, COS-7 cells were transfected as indicated with 50 ng/well of vector encoding WT PLCγ$_2$ (*γ$_2$WT*) or PLCγ$_2$S707Y (*γ$_2$S707Y*) and increasing amounts (0–450 ng/well) of vector encoding BTKE41K/K430R or BTKK430R. *Right panel*, COS-7 cells were transfected as indicated with 1.33 μg/well of vector encoding PLCγ$_2$S707Y (*γ$_2$S707Y*) and 0.66 μg/well of vector encoding WT BTK or BTK harboring the E41K or K430R mutations. Twenty four hours after transfection, the cells were incubated for 18 h with either solvent (*Co.*), 1 μM ibrutinib (*Ibru.*), or 1 μM acalabrutinib (*Acal.*). The cells were lysed, and immunoblotting was performed as indicated using an antibody reactive against the c-Myc epitope present on PLCγ$_2$S707Y, antibody reactive against BTK, antibody reactive against phosphorylated tyrosine on PLCγ$_2$ at position 759 (*pY^{759}*), antibody reactive against phosphorylated tyrosine on PLCγ$_2$ at position 1217 (*pY^{1217}*), or antibody detecting tyrosine phosphorylated proteins in all species (*pY*). *D,* cells from one well each functionally analyzed in *C* were washed with 0.2 ml of Dulbecco's PBS and then lysed by addition of 100 μl of SDS-PAGE sample preparation buffer. Aliquots of the samples were subjected to SDS-PAGE, and immunoblotting was performed using an antibody reactive against the c-Myc epitope present on WT PLCγ$_2$ and PLCγ$_2$S707Y (*a–c*), antibody reactive against BTK (*d–f*), or antibody reactive against β-actin (*g–i*). *E,* COS-7 cells were transfected as indicated with 50 ng/well of vector encoding WT PLCγ$_2$ (*γ$_2$WT*) or PLCγ$_2$S707Y (*γ$_2$S707Y*) and increasing amounts (0–450 ng/well) of vector encoding BTKE41K/R525Q or BTKE41K/ΔKinase (*BTKE41K/ΔKin*). *F,* cells from one well each functionally analyzed in *E* were washed with 0.2 ml of Dulbecco's PBS and then lysed by addition of 100 μl of SDS-PAGE sample preparation buffer. Aliquots of the samples were subjected to SDS-PAGE and immunoblotting was performed using an antibody reactive against the c-Myc epitope present on WT PLCγ$_2$ and PLCγ$_2$S707Y (*a–c*), antibody reactive against BTK (*d–f*), or antibody reactive against β-actin (*g–i*). *G,* COS-7 cells were transfected as indicated with 150 ng/well of vector encoding WT PLCγ$_2$ (*γ$_2$WT*), 50 ng/well of vector encoding PLCγ$_2$S707Y (*γ$_2$S707Y*), and 100 ng/well of vector encoding BTKE41K or BTKE41K/K430R. Analysis of inositol phosphate formation and treatment with BTK inhibitor was done as in Fig. 1. *A–C*, *E*, and *G* show representative results from three independent experiments each as mean values of three technical replicates.

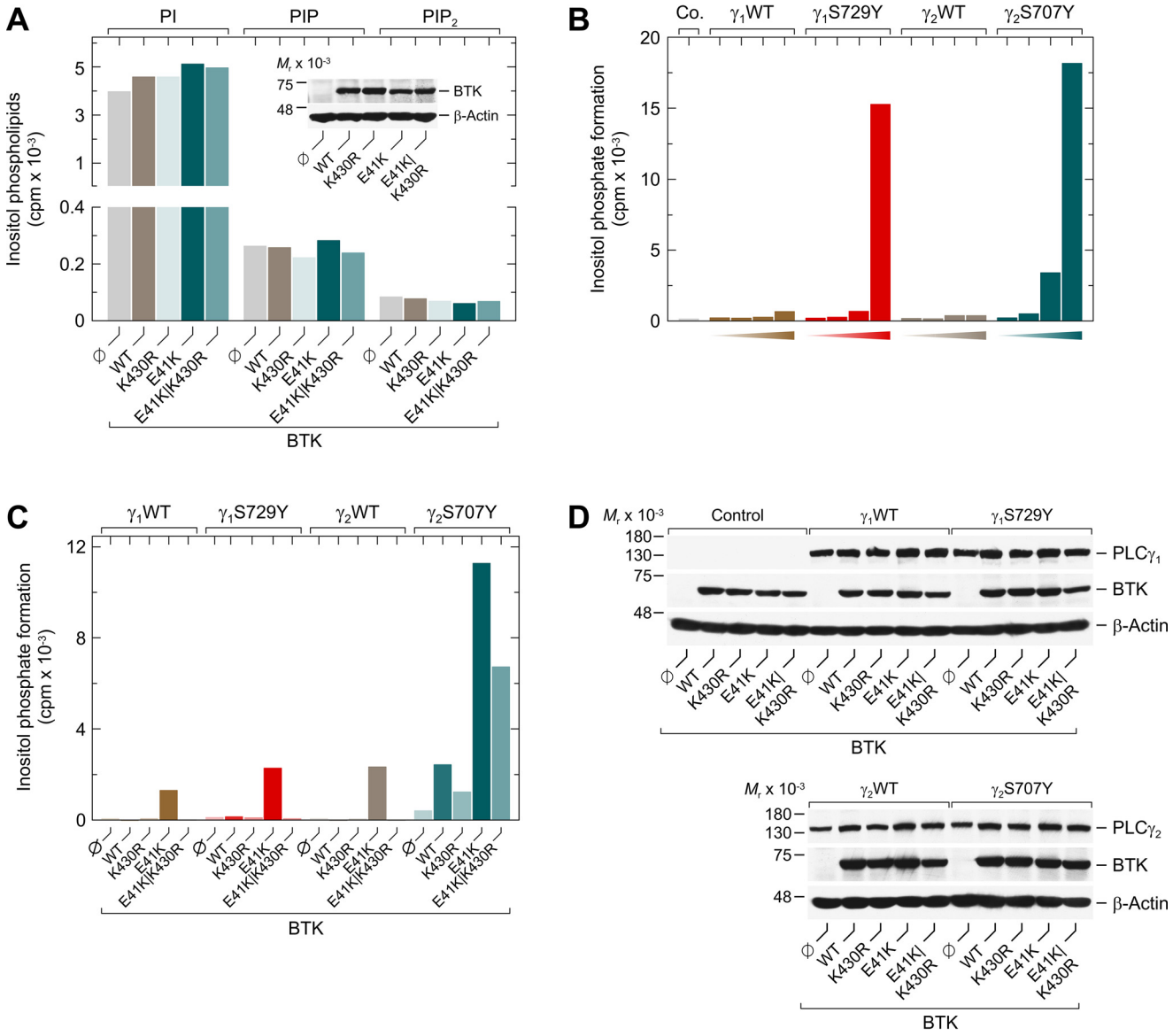

Figure 3. Activation of PLCγ_2S707Y by catalytically-inert BTK is not mediated by augmented PLC substrate availability. *A,* COS-7 cells were transfected as indicated with 2 μg/well of empty vector or 0.5 μg/well of vector encoding WT BTK (*WT*) or BTK variants K430R, E41K, or E41K/K430R. Twenty four hours after transfection, the cells were incubated for 18 h with *myo*-[2-^{3}H]inositol. Then, the amounts of radioactively labeled PtdIns (*PI*), PtdIns*P* (*PIP*), and PtdInsP_2 (*PIP$_2$*) in the intact COS-7 cells were determined by TLC analysis as described under "Experimental procedures." *Inset,* cells from one well each were lysed and subjected to SDS-PAGE. Subsequent immunoblotting was performed using an antibody reactive against BTK or antibody reactive against β-actin. *B,* COS-7 cells were transfected as indicated with 500 ng of empty vector (*Co.*) or increasing amounts (15, 50, 150, or 500 ng) of vector encoding WT PLCγ_1 (γ_1*WT*), PLCγ_1S729Y (γ_1*S729Y*), WT PLCγ_2 (γ_2*WT*), or PLCγ_2S707Y (γ_2*S707Y*). *C,* COS-7 cells were transfected as indicated with 50 ng/well of vectors as described in *B,* and 100 ng/well of vector encoding WT BTK (*WT*) or BTK variants K430R, E41K, or E41K/K430R. Analysis of inositol phosphate formation was done as in Fig. 1. *D,* cells from one well each functionally analyzed in *C* were washed with 0.2 ml of Dulbecco's PBS and then lysed by addition of 100 μl of SDS-PAGE sample preparation buffer. Aliquots of the samples were subjected to SDS-PAGE, and immunoblotting was performed using an antibody reactive against the c-Myc epitope present on WT PLCγ_1, WT PLCγ_2, PLCγ_1S729Y, and PLCγ_2S707Y, antibody reactive against BTK, or antibody reactive against β-actin. *A–C* show representative results from three independent experiments each as mean values of three technical replicates.

phorylation, Tyr-753, Tyr-759, Tyr-1197, and Tyr-1217, and the N-myr–PLCγ_2 carrying an artificial N-terminal signal for myristoylation. The *inset* of Fig. 4 shows that the two variants caused specific enhancements of inositol phosphate formation in intact cells (PLC$\gamma_2$4F < PLCγ_2 <<< PLC$\gamma_2$4E < N-myr-PLCγ_2 < PLCγ_2S707Y). Importantly, a very similar, if not identical, order was observed for the sensitivity of the five PLCγ_2 variants to membrane-targeted BTKE41K, both catalytically-competent and -incompetent. Hence, preactivation of PLCγ_2 appears to predispose the enzyme to further activation by catalytically-inert BTK.

Catalytically-inert BTK causes WT and S707Y variant to differentially interact with the plasma membrane

Next, fluorescence recovery after photobleaching (FRAP) static laser microscopy, employing a fixed-localization Gaussian beam and photon counting to follow fast recoveries (see under "Experimental procedures") (47), was used to investigate the effects of BTKE41K and BTKE41K/K430R on the membrane interaction and diffusion of GFP-tagged WT and S707Y variant PLCγ_2 in intact cells. A significant fraction of PLCγ_2 is cytoplasmic and can therefore recover in FRAP by either lateral

Table 1

Activation of PLCγ$_2$ by catalytically-inert BTK is not limited to PLCγ$_2$S707Y but is also observed for other PLCγ$_2$ variants mediating ibrutinib resistance in CLL cells

COS-7 cells were transfected as indicated with 150 ng/well vector encoding WT PLCγ$_2$ (*PLCγ$_2$WT*); 50 ng/well vector encoding the PLCγ$_2$ variants D334H, R665W, S707Y, S707F, L845F, D993H, and M1141R; 15 ng of vector encoding PLCγ$_2$S707P; and 100 ng/well of vector encoding BTKWT or BTK variants K430R, E41K, or E41K/K430R. The ratios of the PLC activities determined in the presence of BTKE41K/K430R and BTKE41K are specified in the *right column*. The data depicted in the table show representative results from three independent experiments each as mean values of three technical replicates.

BTK	Inositol phosphate formation					Ratio (E41K/K430R: E41K)
	Control	WT	K430R	E41K	E41K/K430R	
			cpm			%
PLCγ$_2$WT	67	86	67	2358	121	5.2
PLCγ$_2$D334H	40	1097	236	10089	4390	43.5
PLCγ$_2$R665W	42	374	138	4420	1956	44.3
PLCγ$_2$S707Y	231	1998	713	17442	8132	46.6
PLCγ$_2$S707F	464	2561	1488	20150	11215	55.7
PLCγ$_2$S707P	728	2991	2563	17734	11584	65.3
PLCγ$_2$L845F	219	1660	455	8937	9668	108.2
PLCγ$_2$D993H	702	3604	1888	10808	7892	73.0
PLCγ$_2$M1141R	1966	5858	5395	14268	14187	99.4

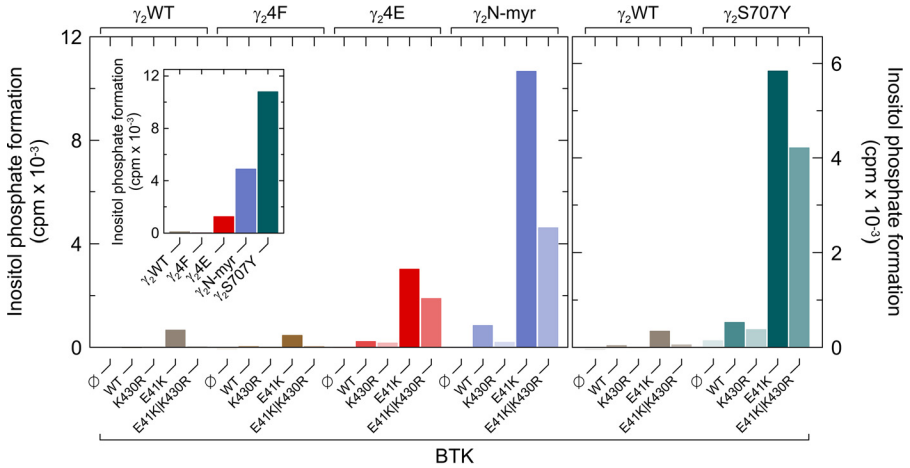

Figure 4. Preactivation of PLCγ$_2$ sensitizes the enzyme to further activation by catalytically-inert BTK. COS-7 cells were transfected as indicated with 50 ng/well of vector encoding WT PLCγ$_2$ (*γ$_2$WT*), PLCγ$_2$4Y→F (*γ$_2$4F*), PLCγ$_2$4Y→E (*γ$_2$4E*), PLCγ$_2$N-myr (*γ$_2$N-myr*) (*left panel*), or PLCγ$_2$S707Y (*γ$_2$S707Y*) (*right panel*) and 100 ng/well of vector encoding WT BTK (*WT*) or BTK variants K430R, E41K, or E41K/K430R. *Inset,* COS-7 cells were transfected as indicated with 500 ng/well of vector to examine the influence of the PLCγ$_2$ mutations on basal inositol phosphate formation in intact transfected cells. Analysis of inositol phosphate formation was done as in Fig. 1. The *graph* shows representative results from three independent experiments as mean values of three technical replicates.

diffusion along the membrane surface or by exchange between membrane-associated and cytoplasmic populations. To evaluate the relative contribution of lateral diffusion and exchange (where the faster process contributes more), we previously developed the FRAP beam-size test (48, 49). This method is based on performing the FRAP experiment using two different laser beam sizes; if the fluorescence recovery is by exchange, the characteristic recovery time (τ) reflects the chemical relaxation time, which is independent of the beam size (48). Under such conditions, the ratio between the τ values measured with the two beam sizes generated in the current experiments by the two objectives equals 1 ($\tau(\times40)/\tau(\times63) = 1$). For lateral diffusion, τ is the characteristic diffusion time τ_D, which is proportional to the area bleached by the beam ($\tau_D = \omega^2/4D$, where ω is the Gaussian radius of the beam, and D is the lateral diffusion coefficient). The results obtained with WT PLCγ$_2$ (Fig. 5) are in line with recovery by lateral diffusion, because the $\tau(\times40)/\tau(\times63)$ ratio (Fig. 5*C*, *leftmost bar*) is not significantly different from 2.28, which is the ratio between the beam sizes generated with these two objectives. However, the D value calculated from the FRAP studies, 3.1 $\mu m^2/s$, is much faster than the D value of a lipid probe $DiIC_{16}(3)$ (1,1′-dihexadecyl-3,3,3′,3′-tetramethylindocarbocyanine perchlorate) in the plasma membrane of the same cells (1 $\mu m^2/s$) (50). This suggests that PLCγ$_2$ membrane interactions are characterized by "gliding" along the inner membrane surface (*i.e.* it dissociates from the membrane but re-associates before it can diffuse away into the cytoplasm). The current results are similar to our earlier FRAP measurements of WT PLCγ$_2$ with the smaller beam size (×63) (49), but we find a somewhat slower recovery with the beam generated by the ×40 objective. Slower recovery suggests stronger interactions with the membrane (because free GFP in the cytosol recovers at a rate faster by at least an order of magnitude). This difference may reflect a higher level of RAC activity in the current measurements, because overexpression of constitutively-active RAC2 increased to a similar level the $\tau(\times40)$ of WT PLCγ$_2$ (49). The effects of coexpressing BTKE41K or BTKE41K/K430R on the membrane interactions of WT PLCγ$_2$–GFP are depicted in Fig. 5*B*, *left panel*. Both BTK variants induced increases in the $\tau(\times40)$ values of WT PLCγ$_2$–GFP and in the $\tau(\times63)$ values; here, the effect of BTKE41K/K430R was weaker. Most importantly, neither of the BTK variants significantly affected the $\tau(\times40)/\tau(\times63)$ ratio of WT PLCγ$_2$–GFP (Fig. 5*C*, *left*), which remained only insignificantly different from the beam-size ratio

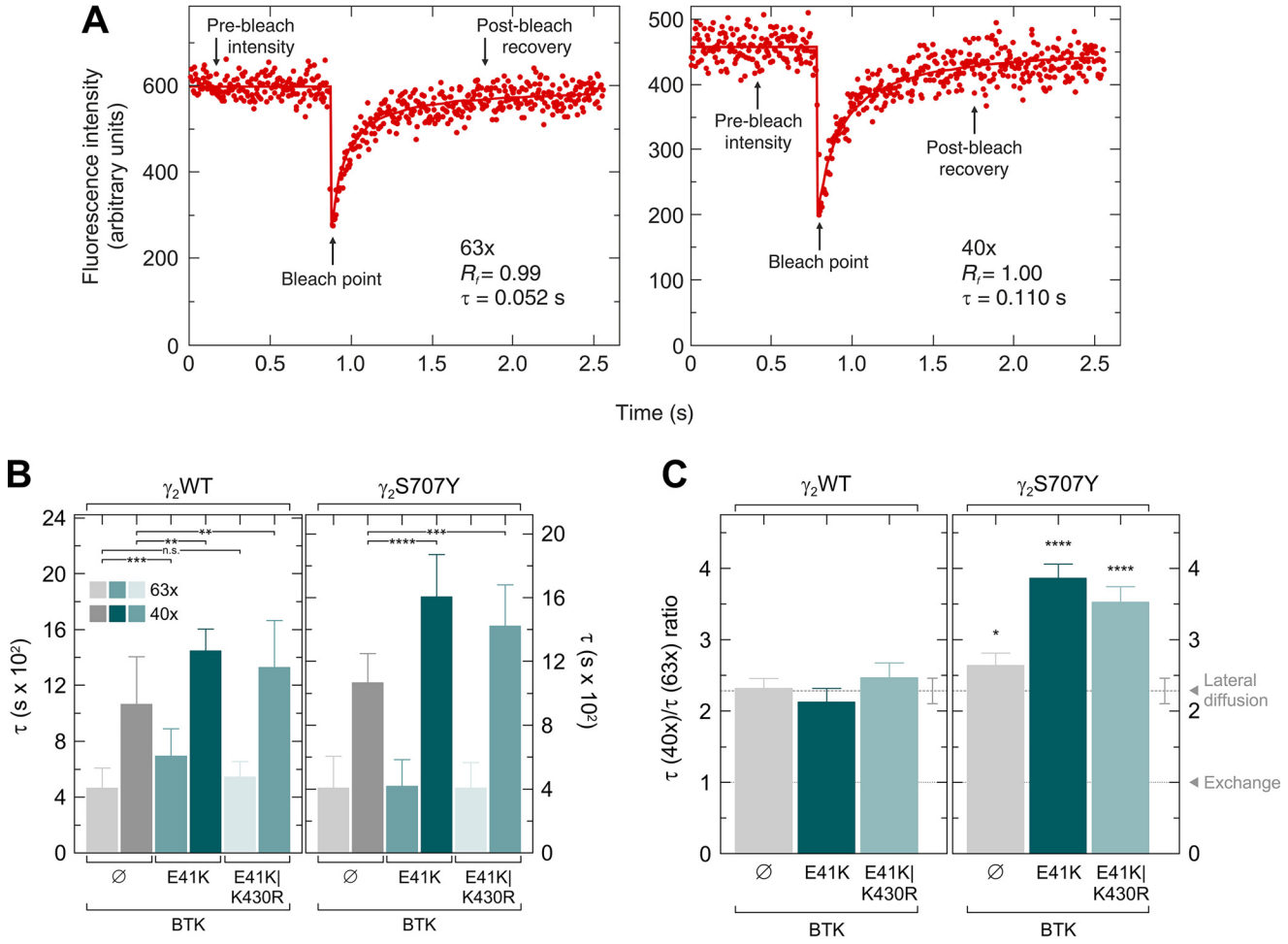

Figure 5. BTK mediates subdiffusion of PLCγ_2S707Y but not of WT PLCγ_2. COS-7 cells were transfected with a vector encoding PLCγ_2–GFP (*γ_2WT*) or PLCγ_2S707Y–GFP (*γ_2S707Y*) together with either empty vector or a vector encoding BTKE41K or BTKE41K/K430R. FRAP studies were conducted 24–26 h post-transfection at 22 °C. *A,* typical FRAP curves obtained using ×63 (smaller beam size) or ×40 (larger beam size) objectives. The time segments showing pre-bleach fluorescence intensity, the bleach point, and post-bleach recovery are indicated by *arrows*. *Solid lines* show the best fit of a nonlinear regression analysis (102), with the resulting τ and mobile fraction (R_f) values. *B* and *C,* FRAP beam-size analysis. *Bars* are means ± S.D. of multiple measurements. The τ data depicted in *B* are also used to calculate the τ ratios shown in *C*. The number of measurements for each condition was as follows: (i) PLCγ_2, ×63 objective, $n = 28$; (ii) ×40 objective, $n = 62$; (iii) PLCγ_2 with BTKE41K, ×63, $n = 24$; (iv) ×40, $n = 22$; (v) PLCγ_2 with BTKE41K/K430R, ×63, $n = 27$; (vi) ×40, $n = 29$; (vii) PLCγ_2S707Y–GFP, ×63, $n = 30$; (viii) ×40, $n = 80$; (ix) PLCγ_2S707Y–GFP with BTKE41K, ×63, $n = 63$; (x) ×40, $n = 58$; (xi) PLCγ_2S707Y–GFP with BTKE41K/K430R, ×63, $n = 58$; and (xii) ×40, $n = 51$. The studies employed ×40 and ×63 objectives, whose beam size measurements ($n = 59$) yielded a ω^2(×40)/ω^2(×63) ratio of 2.28 ± 0.15. Thus, a similar τ(×40)/τ(×63) ratio is expected for FRAP by lateral diffusion. A τ ratio of 1 is expected for recovery by exchange (48). The R_f values were high in all cases (0.98–1.00) and are given in Table S1. *B* displays the τ values, and *C* displays the τ(×40)/τ(×63) ratios. *B*, *asterisks* indicate significant differences between the sample without BTK and the samples with the two BTK variants; the comparison was done separately for the τ(×63) values and the τ(×40) values, comparing the same PLCγ_2–GFP protein without BTK and with one of the BTK variants (*n.s.*, not significant; **, $p < 5 \times 10^{-3}$; ***, $p < 10^{-5}$; ****, $p < 10^{-10}$; one-way ANOVA and Bonferroni post hoc test). *C*, bootstrap analysis (see under "Experimental procedures"; 1000 bootstrap resampling values for both τ and beam-size values) shows that the τ ratio of PLCγ_2 (WT or the S707Y variant) in the absence of BTK fits FRAP by lateral diffusion. In the presence of BTK (either E41K or E41K/K430R), the τ ratio of PLCγ_2S707Y, but not of WT PLCγ_2, becomes significantly higher than the 2.28 beam size ratio (*, $p < 0.05$; ****, $p < 10^{-20}$; bootstrap analysis and Student's two-tailed *t* test). The source data for the FRAP studies containing statistics (*B* and *C*) are provided in Table S1.

throughout (2.28). This suggests that the mechanism of the FRAP remains by gliding, albeit with somewhat enhanced interactions with the membrane, as suggested by the larger τ values. We then compared the membrane interactions of PLCγ_2S707Y–GFP with those of the WT enzyme (Fig. 5*B*, *right panel*). The FRAP results for this variant in the absence of BTK resembled those obtained for WT PLCγ_2–GFP, suggesting recovery by gliding lateral diffusion. However, expression of BTKE41K or BTKE41K/K430R had a markedly different effect than in the case of WT PLCγ_2. Here, only the τ(×40) values of PLCγ_2S707Y–GFP became larger (slower recovery kinetics), resulting in a highly-significant deviation of the τ(×40)/τ(×63) ratio from the 2.28 beam-size ratio expected for recovery by lateral diffusion (Fig. 5*C*, *right panel*). The τ ratio dramatically increased, to 3.6–3.8, suggesting that the recovery becomes slower than expected for lateral diffusion with increasing distances. Such a phenomenon, termed subdiffusion or hop diffusion, may arise due to sensing of membrane heterogeneity by the diffusing molecule, which may reflect phase separation, potentially assisted by the cytoskeleton (51, 52). This indicates that the interactions of the variant PLCγ_2S707Y with membrane heterogeneities, which give rise to the anomalous diffusion, are enhanced by BTK to a much higher degree than those of WT PLCγ_2. Of note, BTKE41K and BTKE41K/K430R had a similar effect, indicating that the effect on PLCγ_2S707Y–GFP arises due to

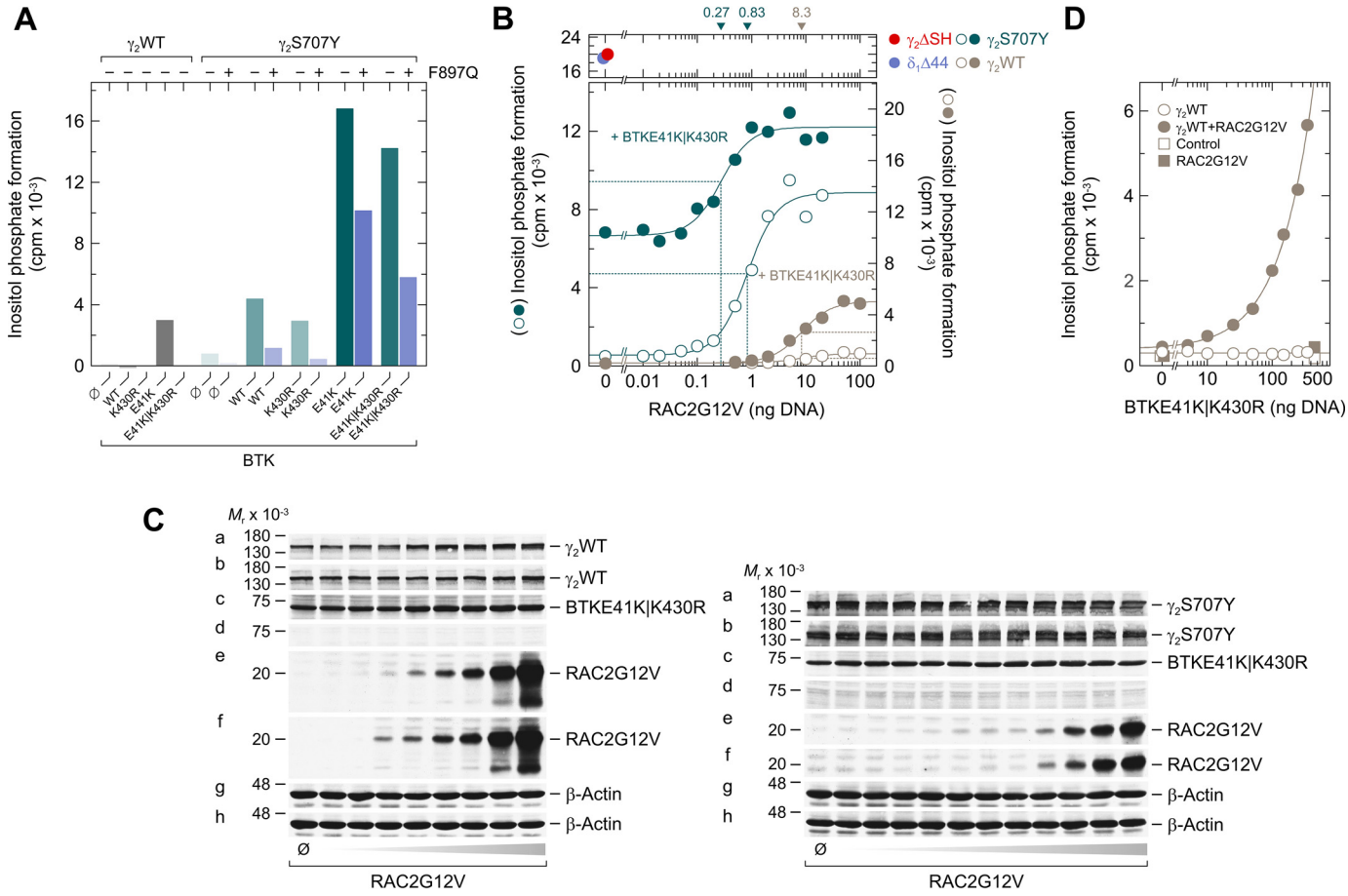

Figure 6. Stimulation via RAC2 augments the responsiveness of the PLCγ$_2$ enzyme to catalytically-inert BTK. *A,* COS-7 cells were transfected as indicated with 50 ng/well of vector encoding WT PLCγ$_2$ (*γ$_2$WT*), PLCγ$_2$S707Y (*γ$_2$S707Y*), and PLCγ$_2$S707Y containing a Phe → Gln mutation at position 897, providing resistance toward RAC2 stimulation (*F897Q*) and 100 ng/well of vector encoding WT BTK (*WT*) or BTK variants K430R, E41K, or E41K/K430R. *B, lower panel*, COS-7 cells were transfected as indicated with 50 ng/well of vector encoding WT PLCγ$_2$ (*γ$_2$WT*) and BTKE41K/K430R or 25 ng/well of vector encoding PLCγ$_2$S707Y (*γ$_2$S707Y*) or increasing amounts (0–100 ng/well) of vector encoding RAC2G12V. *Upper panel*, COS-7 cells were transfected as indicated with 250 ng/well of vector encoding PLCδ$_1$Δ44 (*δ$_1$Δ44*) or PLCγ$_2$ΔSH (*γ$_2$ΔSH*). The ED$_{50}$ values of vector encoding RAC2G12V for the stimulation of WT and variant PLCγ$_2$ activity obtained by nonlinear curve fitting are shown *above the graphs* in ng/well. *C,* cells from one well each functionally analyzed in *B* were washed with 0.2 ml of Dulbecco's PBS and then lysed by addition of 100 μl of SDS-PAGE sample preparation buffer. Aliquots of the samples were subjected to SDS-PAGE, and immunoblotting was performed using an antibody reactive against the c-Myc epitope (*a–b*) present on WT PLCγ$_2$ and PLCγ$_2$S707Y, antibody reactive against BTK (*c–d*), antibody reactive against RAC2 (*e–f*), or antibody reactive against β-actin (*g–h*). *D,* COS-7 cells were transfected as indicated with 50 ng/well of vector encoding WT PLCγ$_2$ (*γ$_2$WT*) and RAC2G12V or increasing amounts (0–350 ng/well) of vector encoding BTKE41K/K430R. Analysis of inositol phosphate formation was done as in Fig. 1. *A*, *B*, and *D* show representative results from three independent experiments each as mean values of three technical replicates.

interactions of BTK with the enzyme, but it does not require BTK tyrosine kinase activity.

Activated RAC2 allows catalytically-inert BTK to activate WT PLCγ$_2$

The previous demonstration that PLCγ$_2$ variants mediating ibrutinib resistance in CLL, PLCγ$_2$R665W, and PLCγ$_2$L845F are hypersensitive to activated RAC endogenously present in COS-7 cells (38) prompted us to determine the contribution of RAC to the effects of catalytically-competent and -incompetent BTK on PLCγ$_2$S707Y. Fig. 6*A* shows that blocking the functional interaction of PLCγ$_2$S707Y with activated RAC in variant PLCγ$_2$–F897Q caused conspicuous losses of inositol phosphate formation, which were particularly striking for the catalytically-inert BTK variants K430R (~85%) and E41K/K430R (~58%). Because the F897Q mutation, located in the C-terminal half of the split PH domain of PLCγ$_2$, is known to neither affect the overall three-dimensional structure of the PH domain nor the catalytic activity of PLCγ$_2$ *in vitro* (49, 53, 54), these results indicate that activated RAC may facilitate BTK-mediated PLCγ$_2$ stimulation, in particular through the noncatalytic functions of BTK. Fig. 6*B* shows that the cellular abundance of exogenous, activated RAC2G12 exerts impressive effects on the activation of both WT and S707Y variant PLCγ$_2$ by catalytically-inert BTKE41K/K430R. Thus, PLCγ$_2$S707Y not only shows higher activity in the presence of RAC2G12V and catalytically-inactive BTKE41K/K430R, but also reveals a higher sensitivity to RAC2G12V in the presence of the latter. The basal activities of the constitutively-active PLC variants PLCγ$_2$ΔSH (lacking the complete autoinhibitory SH2–SH2–SH3 tandem (55)) and PLCδ$_1$Δ44 are shown in Fig. 6*B*, *top panel,* to demonstrate that the plateau observed for PLCγ$_2$S707Y in the presence of BTKE41K/K430R at high RAC2G12V levels is not limited due to exhaustion of the enzyme substrate PtdInsP_2. Increasing concentrations of RAC2G12V had no effect on the expression of PLCγ$_2$ and BTKE41K/K430R (Fig. 6*C*).

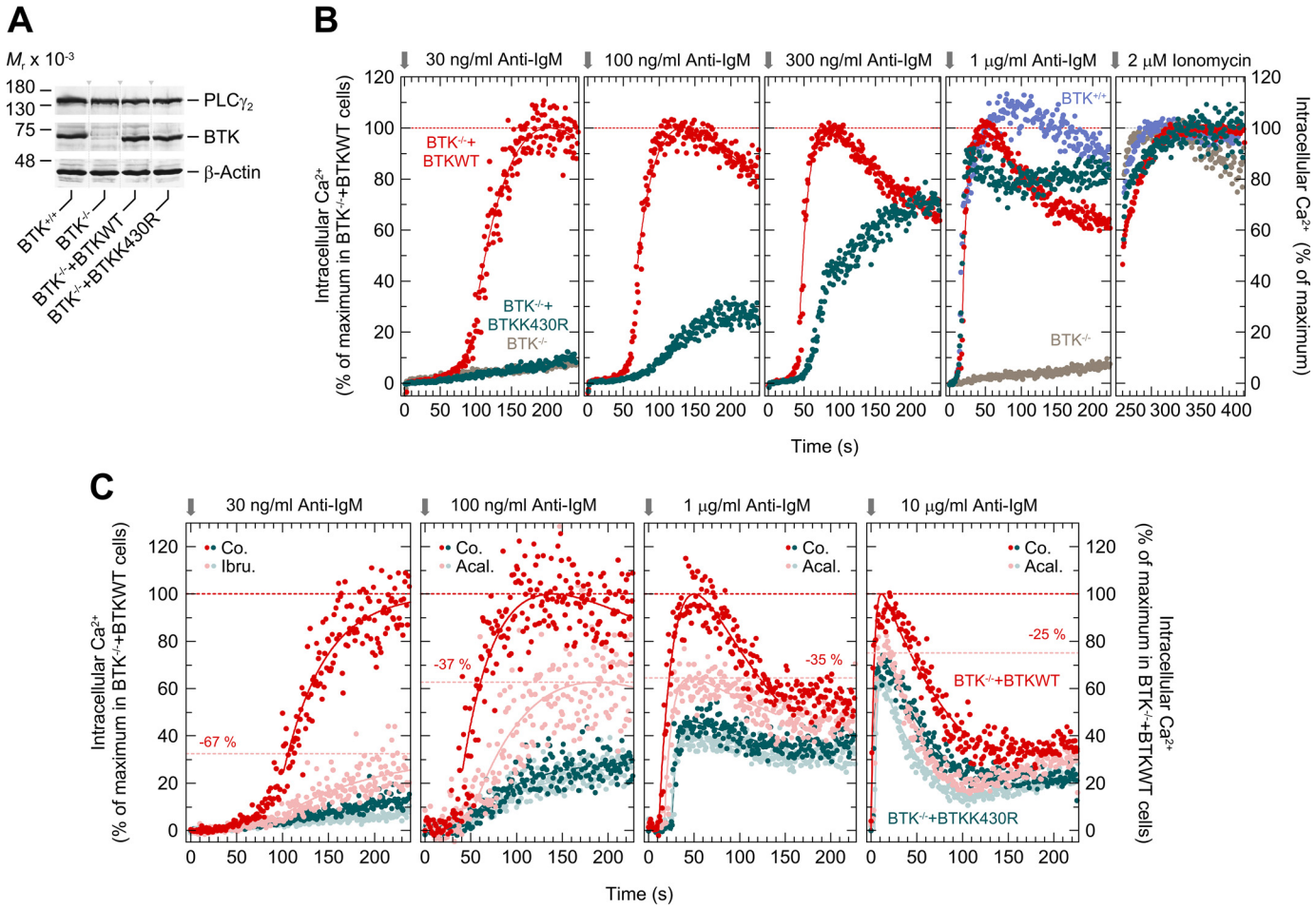

Figure 7. Ability of catalytically-inert BTK to mediate intracellular Ca^{2+} mobilization depends on the level of BCR stimulation. *A*, DT40 cells (1.5×10^6) were lysed as described under "Experimental procedures," and aliquots of the samples were subjected to SDS-PAGE, and immunoblotting was performed using an antibody reactive against both human and chicken BTK, antibody reactive against human and chicken PLCγ_2, or antibody reactive against β-actin. One *empty lane* was present between each of the four lanes from the same immunoblot with the same length of exposure time. These lanes were removed by splicing. The positions of the splice sites are indicated by *gray dotted lines* and *arrowheads*. *B*, WT DT40 cells (*BTK*$^{+/+}$), DT40 BTK$^{-/-}$ (*BTK*$^{-/-}$), and DT40 BTK$^{-/-}$ cells expressing either human WT (*BTK*$^{-/-}$+*BTKWT*) or human K430R BTK (*BTK*$^{-/-}$+*BTKK430R*) were loaded with Indo-1-AM. After pre-warming to 37 °C, the cells were applied to the fluorescence analyzer and treated with anti-IgM followed by ionomycin as described under "Experimental procedures." *C*, DT40 BTK$^{-/-}$ cells expressing either human WT (*BTK*$^{-/-}$+*BTKWT*) or human K430R BTK (*BTK*$^{-/-}$+*BTKK430R*) were either left unstained (*BTK*$^{-/-}$+*BTKWT*) or stained with CFSE (*BTK*$^{-/-}$+*BTKK430R*). After mixing the two populations at a 1:1 ratio, the cells were incubated for 1 h at 37 °C in the presence of either solvent (0.1% (v/v) of DMSO, *Co.*), or 1 μM ibrutinib (*Ibr.*), or acalabrutinib (*Aca.*) followed by washout. Afterward, cells were incubated with indo-1-AM, and the changes in $[Ca^{2+}]_i$ were analyzed as described above. The individual points shown in *B* and *C* correspond to the times in full seconds *versus* the medians of all fluorescence ratios representing $[Ca^{2+}]_i$, following their correction for basal fluorescence intensity in the absence of anti-IgM and normalization according to the maximal values reached after addition of 2 μM ionomycin. In PLC$\gamma_2^{-/-}$ DT40 cells expressing WT PLCγ_2, type M4 anti-IgM causes BCR-mediated increases of $[Ca^{2+}]_i$ at EC_{50} values between 30 and 50 ng/ml (49). Hence, there were no substantial changes in the $[Ca^{2+}]_i$ responses in BTK$^{-/-}$ cells expressing WT BTK when the concentration of anti-IgM was increased to values higher than 30 ng/ml. Specifically, the values were 32.6, 42.9, 35.9, and 28.0% of the maximal Ca^{2+} concentrations upon addition of ionomycin following the addition of anti-IgM at concentrations of 30, 100, and 300 ng/ml and 1 μg/ml, respectively, in *B*), and 28.5, 18.0, 32.8, and 45.4% following the addition of anti-IgM at concentrations of 30 and 100 ng/ml and of 1 and 10 μg/ml, respectively, in *C*).

Strikingly, however, RAC2G12V appeared to unmask a conspicuous sensitivity of WT PLCγ_2 to stimulation by the tyrosine phosphorylation–independent functions of BTK. This strikingly permissive effect of RAC is substantiated by the results shown in Fig. 6*D*, demonstrating insensitivity of PLCγ_2 to BTKE41K/K430R in the absence of RAC2G12V, but with an ~25-fold stimulation of inositol phosphate formation in its presence. The latter results indicate that coactivation of BTK and RAC by upstream regulators may render even WT PLCγ_2 sensitive to the noncatalytic functions of BTK and, by extension, render WT BTK and WT PLCγ_2 at least partially resistant to active-site inhibitors of BTK.

The ability of catalytically-inert BTK to mediate BCR-dependent Ca^{2+} mobilization in intact DT40 B-lymphoma cells is conditional on the degree of BCR stimulation

To investigate the functional significance of the catalytic functions of BTK, the WT enzyme and its catalytically-inactive variant BTKK430R were stably expressed in BTK-deficient DT40 B-lymphoma cells. Fig. 7*A* shows that BTK$^{-/-}$ cells lack immunoreactive BTK protein and that the two reconstituted cells lines, BTK$^{-/-}$+BTKWT and BTK$^{-/-}$ + BTKK430R, express BTK at levels very similar, if not identical, to each other and to unmodified DT40 BTK$^{+/+}$ cells. Fig. 7, *B* and *C*, shows the changes of intracellular free Ca^{2+} in response to increasing concentrations of anti-IgM, as determined by flow cytometry

followed by statistical analysis of the results to allow for direct, quantitative comparison between the different experimental conditions. The *most-right panel* of Fig. 7*B* shows how the maximal Ca^{2+} concentration in response to 2 μM ionomycin was used to correct the traces shown in the other panels for differences in fluorescent dye loading. The corrected traces were then normalized to the maximal Ca^{2+} concentrations observed in $BTK^{-/-}$ + BTKWT cells (100%). Fig. 7*B* shows that there was little, if any, effect of anti-IgM in $BTK^{-/-}$ + BTKK430R cells compared with $BTK^{-/-}$ cells upon addition of anti-IgM at the lowest concentration, 30 ng/ml. Raising the concentration of anti-IgM over 100 and 300 ng/ml to 1000 ng/ml led to a gradual, distinct increase in the ability of the receptor ligand to increase free Ca^{2+}. In addition, there was a progressive loss of the differences in the lag time of the Ca^{2+} responses from about ~35 s at 100 ng/ml anti-IgM and ~20 s at 300 ng/ml, such that there were only relatively minor differences in the kinetics of the Ca^{2+} responses at 1000 ng/ml anti-IgM between the two genetically-modified cell lines and unmodified $BTK^{+/+}$ cells, both in terms of the lag time and the maximal Ca^{2+} concentrations. The results show that the ability of catalytically-inert BTK to mediate BCR-mediated increases in intracellular Ca^{2+} is conditional on the concentration of the BCR ligand, anti-IgM, ranging from no to very sizable responses between 30 and 1000 ng/ml of anti-IgM.

Because the actions of catalytically-inert BTKK430R are insensitive to catalytic site BTK inhibitors like ibrutinib or acalabrutinib (see above), the relative inhibitory effect of these drugs was tested as a function of the degree of BCR activation by anti-IgM. Fig. 7*C*, *most left panel*, shows that ibrutinib (1 μM) caused an ~67% decrease in the maximum Ca^{2+} response in cells expressing WT BTK at the lowest anti-IgM concentration, 30 ng/ml, very close to the Ca^{2+} concentrations observed for cells expressing BTKK430R. In addition, there was a slight inhibitory effect of the drug in the latter cells, presumably due to the known off-target effects of ibrutinib (56). Therefore, acalabrutinib, with less off-target effects than ibrutinib (56), was used. It is evident from the comparison shown in Fig. 7*C* that, at increasing anti-IgM concentrations, not only was there a gradual increase in the ability of catalytically-inert BTK to reconstitute BCR-mediated Ca^{2+} increases, as before, but that, at the same time, there was a quantitative loss to BTK catalytic site inhibition, down to only ~25% in the presence of the maximal anti-IgM concentration tested, 10 μg/ml. In addition, less inhibition at high-ligand concentrations also coincided with a continuous loss of the lag time of the Ca^{2+} response in $BTK^{-/-}$ + BTKWT cells in the absence *versus* presence of the BTK inhibitor. In other words, both the inhibitory efficacy and the kinetic effects on $[Ca^{2+}]_i$ of BTK catalytic site inhibitors were found to be both conditional on and inversely related to the degree of BCR stimulation.

Discussion

Although the molecular basis of clinical resistance to BTK inhibitors, such as ibrutinib and acalabrutinib, caused by mutations at position Cys-481 of BTK are relatively clear, the mechanism of resistance caused by the other *BTK* and the *PLCG2* mutations is less understood. Although *PLCG2* mutations have been suggested to constitute, as a whole, gain-of-function mutations (40, 45, 57), we have previously found that several PLCγ$_2$ variant enzymes carrying mutations in various regions are not constitutively active when assayed in cell-free systems (38, 39). The observation that these PLCγ$_2$ variants are, instead, hypersensitive in intact cells to the Rho GTPase RAC2 led us to suggest that the *PLCG2* mutations found in BTK inhibitor–resistant CLL cells may cause a rerouting of the transmembrane signals emanating from BCR and converging on as well as activating PLCγ$_2$ (38, 39). In addition, Liu *et al.* (40) showed that PLCγ$_2$R665W is sensitive to activation by the proximal tyrosine kinases SYK and LYN even in BTK-deficient chicken DT40 B cells. Even in the presence of BTK, PLCγ$_2$R665W appeared to be resistant to ibrutinib in this system.

Here, we have established a reconstituted system allowing us to monitor the functional interaction of WT and variant forms of BTK and PLCγ$_2$ in intact cells, placing special emphasis on a comparison between WT PLCγ$_2$ and variants known to mediate clinical BTK inhibitor resistance in CLL patients. Although BTK has long been known to mediate protein tyrosine phosphorylation of PLCγ$_2$ following coexpression in cells or cell-free preparations devoid of BLNK (58–60), information on the structural and functional requirements of this interaction to occur and result in enhanced PLCγ$_2$ enzyme activity is limited. This is presumably due to the known requirement of the adaptor protein BLNK to observe BCR-mediated, BTK-dependent activation of PLCγ$_2$ in B cells (61), together with the known difficulties to functionally reconstitute all three components outside the B cells context.

Our findings reveal that functional interaction of BTK and PLCγ$_2$ in a non-B-cell environment is conditional on the introduction of mutations into the two coding regions and on the level of protein expression. Thus, although there was no productive interaction between the two WT components even at the highest expression level of BTK, mutational alteration of either PLCγ$_2$ (S707Y) or BTK (E41K), or both, caused profound increases in PLCγ$_2$ activity. The results obtained on WT PLCγ$_2$ are consistent with the view that one of the roles of BLNK is to provide membrane targeting to PLCγ$_2$ to make it more susceptible to BTK-mediated protein tyrosine phosphorylation. In fact, a membrane-targeted variant of PLCγ$_2$ was sensitive to BCR stimulation even in the absence of BLNK (62, 63). According to this view, membrane targeting of BTK, such as introduced by the E41K mutation, would serve the same purpose. Extrapolating this concept to the altered functional properties of PLCγ$_2$S707Y, which is highly sensitive to stimulation by even WT BTK, could indicate that this PLCγ$_2$ variant may also be different from the WT enzyme in its membrane interaction.

The marked sensitivity of the functional BTKE41K–PLCγ$_2$WT interaction to BTK inhibitors of all three generations shows that the protein kinase activity of BTKE41K is an important determinant of this interaction; phosphoblot analysis shows that PLCγ$_2$ is a likely substrate of this activity. However, comparison of PLCγ$_2$WT and PLCγ$_2$S707Y revealed, unexpectedly, a fundamentally different dependence on protein tyrosine phosphorylation of the two PLCγ$_2$ isoforms. Thus, the catalytically-inactive forms of BTKE41K and even BTKWT were clearly capable of causing marked activation of

PLCγ_2S707Y, but not of PLCγ_2WT, in the absence of apparent protein tyrosine phosphorylation of the PLCγ_2 variant. Importantly, this activity was also observed for another known catalytically-inactive variant of BTK, BTKE41K/R525Q (13), and even by a deletion variant of BTK lacking its catalytic domain.

In the absence of alternative regulatory pathways between BTK and PLCγ_2, as is the case in the cell system employed here for transient functional reconstitution, activation of PLCγ_2, both WT and the various point variants analyzed herein, are, on first approximation, expected to be similarly sensitive to inhibition by active-site inhibitors of BTK. However, as shown in Fig. 2, *A* and *G*, they are not. PLCγ_2S707Y was inhibited by acalabrutinib only to the extent of its activity that depended on the kinase activity of BTKE41K, whereas the remaining activity, which results from BTK catalysis-independent functions, was completely acalabrutinib-resistant. This drug-resistant portion may even be higher for other PLCγ_2 point variants with a higher BTK E41K/K430R:E41K ratio, such as the variants L845F or M1141R (Table 1). This mechanism provides an explanation, at least in part, for active-site BTK inhibitor resistance in tumor cells expressing *PLCG2* point variants, without a requirement for constitutively-enhanced intrinsic activity, which is consistent with previous studies of the R665W and S707Y PLCγ_2 variant proteins *in vitro* (38, 39).

Preactivation of PLCγ_2, regardless whether by phosphomimetic mutations or by membrane targeting at its N terminus (64), rendered the variants hypersensitive to activation by both catalytically-active and -inactive BTK (*cf.* Fig. 4). This effect was particularly striking for the variant carrying the myristoylation tag of Rous sarcoma virus v-SRC at its N terminus, PLCγ_2N-myr, which had a functional phenotype *vis à vis* BTK, WT, and variants, very similar to PLCγ_2S707Y. Importantly, PLCγ_1 phosphorylation and Ca^{2+} release were previously promoted in *Xenopus laevis* egg extracts by lipid rafts prepared from COS-7 cells expressing the *Xenopus* SRC protein, suggesting that COS-7 cells contain lipid raft microdomain structures and that SRC kinase is targeted to these structures (65, 66). Hence, the N-terminal SRC-derived myristoylation tag was likely to promote lipid raft targeting of PLCγ_2N-myr to COS-7 cell lipid rafts. Membrane-targeting tags of lipid raft–associated proteins FcγRIII (62, 67, 68) or the Src family member LYN (63) have previously been attached to PLCγ_2 and found to render BCR-mediated stimulation of PLCγ_2 in DT40 cells independent of the adaptor protein BLNK. The similarity of the functional phenotypes *vis à vis* BTK, WT, as well as variants, between PLCγ_2N-myr and PLCγ_2S707Y (*cf.* Fig. 4) and the hop diffusion in the membrane detected by FRAP for PLCγ_2S707Y in the presence of BTKE41K or BTKE41K/K430R (*cf.* Fig. 5), suggests that the latter protein functionally resembles a lipid raft–associated protein, possibly with acquired BLNK independence of activation by BTK. With regard to the FRAP results, an "anchored membrane-protein picket model" has been proposed by Fujiwara *et al.* (51), in which transmembrane proteins referred to as "pickets" are anchored to the membrane skeleton to act as posts along the membrane skeleton fence. The anchored protein pickets, observed in all examined cell types, including COS cells, were suggested to act as effective diffusion barriers due to steric hindrance as well as circumferential slowing (packing and frictional) effects even for phospholipids in the outer leaf of the membrane. According to this model, the long-range lateral diffusion of diffusible molecules in compartmentalized membranes is largely limited by their hop rate across the compartment boundaries. Importantly, compartmentalization of the cell membrane has also been suggested to occur for glycosylphosphatidylinositol-linked proteins and to be involved in modulating the size and lifetime of lipid rafts. Collectively, the results suggest that the point mutation S707Y promotes association with compartmentalized plasma membrane subdomains, possibly with lipid rafts. The importance of the latter for BCR-mediated signal transduction in B cells has previously been emphasized (69–72).

We have shown earlier that RAC, by physically interacting with the split PH domain of PLCγ_2, amplifies BCR-induced Ca^{2+} signaling and markedly increases the sensitivity of B cells to BCR ligation, BCR-mediated Ca^{2+} release from intracellular stores, Ca^{2+} entry from the extracellular compartment, and nuclear translocation of the Ca^{2+}-regulated nuclear factor of activated T cells (49). We also showed that various PLCγ_2 variants are strikingly hypersensitive to activation by RAC2, such that even WT RAC2 suffices to activate the variant enzymes upon its introduction into intact cells (38, 39). These findings are highly consistent with the cooperative interaction between RAC2 and BTK as stimulators of PLCγ_2 shown here, in particular with the striking permissive effect of activated RAC on the ability of catalytically-inert BTKE41K/K430R to activate even WT PLCγ_2 (*cf.* Fig. 6, *B* and *D*). This result may indicate an "unleashing", via VAV and RAC, of even WT PLCγ_2 activity by the catalysis-independent functions of BTK. This effect could act in *cis, i.e.* within the BCR signal transduction pathway in a positive feed-forward regulatory loop, or in *trans,* via BCR coreceptors or integrins also capable of activating RAC (38), both enhancing BCR-mediated PLCγ_2 activation. In either case, the sensitivity of BCR-mediated inositol phosphate formation to catalytic site–targeted inhibitors of BTK would be dependent on the relative penetrance of the pathways mediated by BTK independently of its protein kinase activity in the various physiological and pathophysiological environments of either normal or leukemic B cells. Of note, both VAV and RAC have been shown to localize to lipid rafts in B cells (70, 73).

An important extracellular variable encountered by B cells in different tissue environments is the abundance of the BCR antigen stimulus and, hence, the degree of BCR activation. The result shown herein indicate that this degree takes a profound influence on both the kinetics of the $[Ca^{2+}]_i$ response and on the portion that may be contributed by the protein-tyrosine kinase–independent functions of BTK, which are resistant to catalytic site-targeted BTK inhibitors. Remarkably, in DT40 cells, this portion increased considerably when the concentration of anti-IgM was increased over the range of concentrations commonly used in the functional analysis of these cells.

At first glance, these findings may appear to contradict earlier seminal findings, such as the almost complete loss of the reconstitutive activity of catalytically-inert BTK variant R525Q in BTK$^{-/-}$ DT40 cells (K$^-$/*btk*$^-$), which was tested in response to type M4 anti-IgM at a nominal concentration of 2 μg/ml (13). Although it seems possible, as pointed out earlier (74), that

the R525Q mutation used by Takata and Kurosaki (13) affects the catalytic capacity of the BTK kinase differently, the three kinase-inactive BTK variants analyzed herein, including the variant R525Q and even lacking the kinase domain, behaved very similarly in our experiments (*cf.* Fig. 2*E*). Notably, however, unlike Lys-430, Arg-525 is not conserved in the protein kinase superfamily and is already absent in this position in most of the human Src subfamily members, including LYN. Finally, in our hands, the anti-IgM concentration response of DT40 cells is sensitive to freezing and storage of the cells and, possibly, storage of the ligand at 4 °C, as well as somewhat variable with the particular batch of the ligand. For example, freshly-transfected cells that had not been frozen as such were used with freshly-prepared ligand in Fig. 7*B*. In Fig. 7*C*, the anti IgM-mediated $[Ca^{2+}]_i$ increases were already reduced, *e.g.* at 1 μg/ml anti-IgM, after one freeze-thaw cycle. Therefore, it seems possible that the observations in Fig. 7*C* did in fact correspond to less-responsive cells and/or a less potent anti-IgM preparation. *In vivo* analysis of genetically-modified mice and experiments performed *ex vivo* on cultured cells from these animals have previously shown that the catalytically-inactive BTK variant K430R could either fully, only partially, only modestly, or not at all fulfill the functions of WT BTK, depending on the particular function tested (23, 24). These results have previously been explained by the finding, in primary and A20 cultured B cells, that BTK, regardless of its catalytic capabilities, associates with PIP5Ks, the enzymes that synthesize PtdInsP_2 (25, 75). The findings were taken by the authors (25) to suggest that both forms of BTK act as shuttles to bring PIP5Ks to the plasma membrane and specifically to lipid rafts to enhance the availability of PtdInsP_2 as a substrate for both PI3 kinases and PLCγ_2 with subsequently enhanced membrane targeting of BTK (via its PH domain) and inositol phosphate formation, respectively. Although such a mechanism(s) appears persuasive, it is important to note that increased formation of PtdInsP_2 by protein kinase– deficient BTK has not been shown in Saito *et al.* (25), neither in anti-IgM–stimulated DT40 cells nor in PIP5Kβ-overexpressing A20 cells. In addition, the observation herein that a number of *PLCG2* point mutations associated with ibrutinib resistance of CLL cells cause markedly enhanced inositol phosphate formation in transfected cells (*cf.* Table 1), arguing strongly against a shortage of substrate PtdInsP_2 at the site of catalysis. Furthermore, even activated BTKE41K did not alter the activity of WT or mutationally preactivated PLCδ_1 in the experimental system utilized here (*cf.* Fig. 1*A*). There was also no change in the levels of the major inositol phospholipids in response to expression of various variant forms of BTK, including those capable of stimulating PLCγ_2S707Y (*cf.* Fig. 3*A*). Finally, and perhaps most convincingly, there was a striking PLC isozyme specificity of the stimulatory effect of catalytically-inactive BTK, even within the PLCγ subfamily, where PLCγ_1S729Y, the direct structural and functional counterpart of PLCγ_2S707Y (39), did not show activation by BTKE41K/K430R (*cf.* Fig. 3*C*). Note that both PLCγ_1 and PLCδ_1 associate with lipid raft membrane microdomains (76, 77), and should, as such, be similarly if not equally sensitive, as compared with PLCγ_2, to an enhanced availability of the PtdInsP_2 substrate.

Tomlinson *et al.* (74) showed earlier that an inducible form of kinase-inactive BTK, in contrast to its kinase-active counterpart, was unable to induce an increase in $[Ca^{2+}]_i$ in BTK-deficient DT40 cells on its own. However, in the context of BCR activation by 2 μg/ml anti-IgM, there was virtually no difference in the kinetics of $[Ca^{2+}]_i$ between BTK$^{-/-}$ cells expressing kinase-active *versus* -inactive BTK. Hence, BCR-mediated activation of PLCγ_2 via kinase-inactive BTK involves an additional mechanism. In the context of the results shown here (*cf.* Fig. 6, *A–D*), it is likely that RAC activated by the BCR, *e.g.* via VAV, permits the implementation of such a mechanism. We previously noted major losses of the proportion of singly analyzed DT40 cells carrying the RAC-resistant PLCγ_2 variant F897Q in response to intermediate and high concentrations of anti-IgM, without an apparent change in the anti-IgM sensitivity of the cells. In addition, the integrated single-cell fluorescence intensities, as well as peak latencies, amplitudes, and frequencies were markedly (mostly up to >80%) reduced in these cells under these conditions (49). We therefore suggest that, following intermediate to high degree BCR activation by antigens, activated RAC physically interacts with WT PLCγ_2 to sensitize the enzyme to the noncatalytic actions of BTK.

Considering the BCR-coupled multiprotein transmembrane-signaling chain as one functional unit coupling a ligand-binding receptor to a second messenger– generating enzyme such as PLCγ_2, catalytic site–targeted BTK inhibitors can be categorized as variably effective, either irreversible (*e.g.* ibrutinib and acalabrutinib) or reversible (*e.g.* vecabrutinib) allosteric inhibitors: allosteric because they act at a site distinct from the (orthosteric) receptor–ligand-binding site. Based on the results presented herein, we suggest that inhibition by ibrutinib and acalabrutinib is only fully expressed at low degrees of BCR activation where only the catalysis-dependent effects of BTK are in effect. At high degrees of BCR activation, more and more of the catalysis-independent BTK functions come into effect, such that the BTK inhibitors acquire the properties of only partially-effective inhibitors. Whether or not the remaining relative inhibition suffices to block specific (patho)biologic functions of BCR depends on the "functional reserve" of the particular B-cell response distal to the increase in $[Ca^{2+}]_i$. In other transmembrane-signaling systems, such as those relying on enhanced intracellular formation of cAMP, this term refers to the fact that many receptor agonists are more powerful than they need to be, in that maximal responses of cellular functions are elicited at submaximal, in some cases only minimal degrees of receptor activation or second messenger generation (78, 79). For example, it is well-known that in adipocytes stimulated by lipolytic hormones the levels of cAMP are far in excess of those required for maximal lipolytic rates, even in the presence of inhibitors (80–82). This large "overshoot" of second messenger is also observed, *e.g.* in the heart and in adrenocortical cells, in many other biological systems with no direct correlation of second messenger concentration with the metabolic or physiological process under investigation (83, 84). Under these conditions, both orthosteric and allosteric inhibitors need to be capable of blocking a substantial portion, if not a great majority, or even all agonist effects to be efficacious (85, 86). Thus, as long as the BCR operates under a functional reserve arrangement in a given

B cell, the changes in BTK inhibitor efficacy shown herein (*cf.* Fig. 7*C*) may take profound effects on and limit their therapeutic efficiency in cells expressing both WT BTK and WT PLCγ_2, in particular at high degrees of BCR activation, as determined by high affinity and/or high abundance of the antigen.

In CLL cells, BCR activation may occur through engagement of the receptor by (auto)antigens (87, 88) or in a cell-autonomous way by BCR recognition of conserved epitopes within specific regions of the Ig heavy and light chains (89, 90). Either way, there are substantial differences in the degrees of this activation among samples of different patients, which in turn translates (at least in part) to the clinical heterogeneity of the disease (90, 91). Importantly, BTK inhibitor treatment of CLL has been reported to be limited by primary drug resistance in 13–30% (10). Partial efficacy of the drugs caused by the activation of PLCγ_2 through catalysis-independent mechanisms of BTK provides a potential mechanism of this therapeutic problem. Novel drugs capable of interfering with the protein–protein interaction(s) of BTK with PLCγ_2 may provide a way to address this treatment drawback in the future. Finally, clinical heterogeneity, referred to as "leaky" or "mild" phenotype in the less affected patients, is also known in XLA, even in patients from single pedigrees. It has previously been difficult or even impossible to establish a clear genotype–phenotype relationship for this disease caused by a large number of distinct mutations in BTK (RRID:SCR_013101). In some cases, these mutations either abrogate the catalytic functions of BTK (92) or cause a loss of its catalytic domain (93). We suggest that the noncatalytic functions of the variant BTK enzymes, possibly triggered in a sibling-specific fashion by high BCR activation, may contribute to this heterogeneity.

Experimental procedures

Materials

The rabbit polyclonal antibody 3872 reactive against human and chicken PLCγ_2, the rabbit polyclonal antibody 3871 reactive against human PLCγ_2 phosphorylated at tyrosine 1217, the rabbit polyclonal antibody 3874 reactive against human PLCγ_2 phosphorylated at tyrosine 759, and the rabbit polyclonal antibody 5082 reactive against human BTK phosphorylated at tyrosine 223 were obtained from Cell Signaling Technology. The rabbit polyclonal antiserum reactive against human RAC2 (sc-96), the mouse mAb reactive against human BTK (sc-81735), and the mouse mAb (PY99) reactive against phosphotyrosine-containing proteins (sc-7020) were purchased from Santa Cruz Biotechnology. The rabbit polyclonal antibody reactive against human and chicken BTK (F52632) was obtained from NSJ Bioreagents. CFSE (eBioscience™, 65-0850-84) and Indo-1-AM (I1223) were obtained from Thermo Fisher Scientific. Mouse anti-chicken IgM (clone M-4) was obtained from Southern Biotech. The BTK inhibitors ibrutinib (PCI-32765) and acalabrutinib (ACP-196) were obtained from Selleckchem. The BTK inhibitor vecabrutinib (SNS-062) was kindly provided by Sunesis. The sources of other reagents have been described in Ref. 39, 94. BTK-deficient DT40 cells were kindly provided by J. Wienands, Institute of Cellular and Molecular Immunology, University of Göttingen.

Construction of vectors

The 4E variant (Y753E, Y759E, Y1197E, and Y1217E) of PLCγ_2 was generated according to the 4F variant. The cDNA encoding PLCγ_2N-myr was generated by N-terminal insertion of the first 15 amino acids from Rous sarcoma virus SRC (MGSSKSKPKDPSQRR) (95) and a small linker (PGIQ) providing a BamHI site into PLCγ_2–pcDNA3.1(+). BTKΔkinase, lacking amino acids 402–659, was generated with help of *in vitro* mutagenesis by insertion of a stop codon (TAG) right in front of the kinase domain. The primer sequences and PCR protocols are available from the authors upon request. The cDNAs of *n*-FLAG epitope-tagged human BTK and its point variants R28C, E41K, Y223F, and K430R were provided by C. Brunner, Department of Otorhinolaryngology, Head and Neck Surgery, Ulm University Medical Center. The BTK variant Y551F was generated by O.-O. Wolz from the Department of Immunology, University of Tübingen. The generation of all other cDNAs has been detailed in Refs. 43, 49, 96.

Generation of stably-transfected DT40 cell clones, DT40 cell culture, and preparation of DT40 cell lysates

This was essentially done as described in Ref. 49. Proteomic analysis of whole-cell extract proteins, fractionated by SDS-PAGE, was used to verify the expression of WT and K430R variant BTK in the respective cell clones as described previously (97). MS/MS spectra were correlated with the UniProt chicken database complemented with the sequences of human WT and K430R variant BTK. Carbamidomethylated cysteine was considered as a fixed modification along with oxidation of methionine, and acetylated protein N termini as variable modifications. False discovery rates were set on both peptide and protein levels to 0.01.

Calcium flux measurements

Cells were suspended at a density of 10^7 cells/ml in FACS buffer (143 mM NaCl, 6 mM KCl, 1 mM $MgSO_4$, 20 mM HEPES/NaOH, pH 7.4, 1 mM $CaCl_2$, 5.6 mM glucose) and incubated for 45 min at 37 °C and 10% CO_2 with 5 μM Indo-1-AM. The calcium measurements were performed on a BD FACS Celesta™. In brief, 10^6 cells per sample in 0.5 ml of FACS buffer were pre-warmed at 37 °C for 10 min. Next, baseline was measured for 2 min before addition of the ligand anti-chicken IgM. After an additional 4 min, 2 μM ionomycin (I0634, Sigma) was added to the samples to obtain the maximal Ca^{2+} flux. Cells were kept at 37 °C during the measurements. The fluorescence ratio of Indo-1 violet (Ca^{2+}-bound) to Indo-1 blue (Ca^{2+}-free) was measured by using FACSDiva™ software (BD Biosciences). In some cases, two cell populations were analyzed simultaneously by staining half of the cells for 10 min at 37 °C and 10% CO_2 with 20 nM CFSE (98), followed by washing of the cells (10^7 cells/ml) with 10 volumes of PBS. For BTK inhibitor treatment, unstained and CFSE-labeled DT40 cells were treated for 1 h at 37 °C with continuous shaking at a density of 10^7 cells/ml with 1 μM inhibitor or solvent in RPMI 1640 medium containing supplements. The inhibitor was washed out before adding the Ca^{2+} indicator. For data evaluation, the experimental results contained in FCS files generated by the FACSDiva™ software (BD Biosciences) were imported into the FlowPy Python tool

(RRID:SCR_018195) and then transferred to Excel spread sheets. Following binning of the time attributes of the individual data points to integers (full seconds), the data of one experiment were assembled into a matrix M such that the first row listed the time attributes and the columns j in rows i + 1 tabulated the fluorescence ratios. The resulting matrices were typically made up of about 540 columns and up to about 1650 rows. In experiments analyzing two cell populations at the same time, DT40 cells expressing WT BTK (unstained) and DT40 cells expressing BTKK430R (stained) (Fig. 7*C*), the matrix was fractionated into two parts, M1 and M2, according to the fluorescence intensities determined for intracellular CFSE. The individual points shown in Fig. 7, *B* and *C,* correspond to the times in full seconds *versus* the medians of all fluorescence ratios representing $[Ca^{2+}]_i$, following their correction for basal fluorescence intensity in the absence of anti-IgM and normalization according to the maximal values reached after addition of 2 μM ionomycin. Between serial measurements, the latter values were normalized to 100%. Nonlinear least-squares curve fitting of selected portions of the data to equations of either one-phase exponential association, two-exponential association and decay, or log-normal distributions was done using GraphPad Prism®, versions 8.2.1 or 4.03, to determine the values corresponding to the maximal $[Ca^{2+}]_i$ concentrations for normalization to allow for quantitative comparison between experiments.

Cell culture and transfection of COS-7 cells, extraction, and analysis of inositol phospholipids

This was done as described previously (38, 39, 53, 55, 99).

Radiolabeling of inositol phospholipids and analysis of inositol phosphate formation

Twenty four hours after transfection, COS-7 cells were washed once with 0.3 ml/well of Dulbecco's PBS (PAA Laboratories) and then incubated for 18 h in 0.2 ml/well DMEM-containing supplements, as described previously (38), supplemented with 2.5 μCi/ml *myo*-[2-^{3}H]inositol (NET1156005MC, PerkinElmer Life Sciences), and 10 mM LiCl. The cells were then washed once with 0.2 ml/well Dulbecco's PBS and lysed by addition of 0.2 ml/well 10 mM ice-cold formic acid. The analysis of inositol phosphate formation was performed as described previously (53) except that 15 ml of scintillation fluid Quicksafe A from Zinsser Analytic was used. To examine BTK inhibition via ibrutinib, acalabrutinib, or vecabrutinib, COS-7 cells were radiolabeled for 18 h in 0.2 ml/well DMEM-containing supplements as described previously (38), supplemented with 2.5 μCi/ml *myo*-[2-^{3}H]inositol, 10 mM LiCl, 0.1% v/v DMSO (D2650, Sigma) or the respective BTK inhibitor.

Phosphoblot analysis

COS-7 cells were seeded into 6-well plates and transfected. After an additional medium change, the cells were incubated for a further 18 h at 37 °C and 10% CO_2. The medium was removed, and the cells were washed with 0.5 ml of ice-cold TBS and then lysed by addition of 250 μl of phospholysis buffer (25 mM Tris-HCl, 100 mM NaCl, 1 mM EDTA, 0.5% (v/v) NP40, 0.2% (v/v) Triton X-100, 5% (v/v) glycerol, pH 7.5) supplemented with protease inhibitors (1 mM phenylmethylsulfonyl fluoride, 10 μM leupeptin, 2 μM pepstatin A, 2 μg/ml soybean trypsin inhibitor, 1 μg/ml aprotinin, and 3 mM benzamidine) and phosphatase inhibitors (2 mM sodium orthovanadate, 9.5 mM sodium fluoride, 10 mM β-glycerophosphate, and 10 mM tetrasodium pyrophosphate). After lysis, 250 μl of 2× SDS-PAGE sample preparation buffer were added, and aliquots of the samples were subjected to SDS-PAGE followed by immunoblotting.

FRAP experiments

FRAP studies (100, 101) were conducted as described earlier (49), using a fixed-localization Gaussian laser beam focused to a very small spot on the membrane for both bleaching and monitoring, continuously measuring the fluorescence intensity at the spot by photon counting (47). This method gives a much better time resolution (down to a few milliseconds) than FRAP of larger regions-of-interest in a confocal microscope, which employs nonsynchronous stepwise bleaching and monitoring, which take significantly longer (47). The improved time resolution is critical in the case of fast recovery contributed by exchange and/or gliding, as is the case in this study. The experiments were performed 24–26 h post-transfection on COS-7 cells transfected with PLCγ_2–GFP derivatives. All experiments were conducted at 22 °C, in Hanks' balanced salt solution supplemented with 20 mM HEPES/NaOH, pH 7.2. The monitoring argon ion laser beam (488 nm, 1.2 microwatts; Innova 70C, Coherent) was focused through the microscope (AxioImager.D1, Carl Zeiss MicroImaging) to a Gaussian spot with a radius $\omega = 0.77 \pm 0.03$ μm (×63/1.4 NA oil-immersion objective) or 1.17 ± 0.05 μm (×40/1.2 NA water immersion objective). Experiments were conducted with each beam size (beam size analysis is described in Refs. 48, 49). The ratio between the illuminated areas ($\omega^2(\times40)/\omega^2(\times63)$) was 2.28 ± 0.15 ($n = 59$; S.D. calculated using bootstrap analysis as described below). After a brief measurement at the monitoring intensity, a 5-milliwatt pulse (4–6 or 10–20 ms for the ×63 and ×40xobjectives, respectively) bleached 50–70% of the fluorescence in the illuminated spot. Fluorescence recovery was followed by the monitoring beam. The apparent characteristic fluorescence recovery time (τ) and the mobile fraction (R_f) were derived from the FRAP curves by nonlinear regression analysis, fitting to a lateral diffusion process with a single τ value (102). The significance of differences between sets of τ values measured with the same beam size was evaluated by one-way ANOVA and Bonferroni post hoc test. To compare the $\tau(\times40)/\tau(\times63)$ ratio of a given PLCγ_2 variant with the $\omega^2(\times40)/\omega^2(\times63)$ beam-size ratio (comparing a single pair of data sets), statistical significance was evaluated by two-tailed Student's *t* test using bootstrap analysis with 1000 bootstrap samples (103), which is preferable for comparison between ratios, as described by us previously (104).

Miscellaneous

SDS-PAGE and immunoblotting were performed according to standard protocols using antibodies reactive against the c-Myc epitope for WT and variant PLCγ_1, PLCγ_2, and PLCδ_1 or antibodies reactive against BTK, PLCβ_2, RAC2, and β-actin. Immunoreactive proteins were visualized using the Pierce ECL Western blotting detection system (catalog 32106, Thermo

Fisher Scientific). Samples to be analyzed by Western blotting were taken, *quasi* as a fourth replicate, from the same plate as and immediately adjacent to the samples taken in triplicate for functional analysis. Using this protocol and paying meticulous attention to experimental detail, we were able to demonstrate for all results obtained in transiently-transfected COS-7 cells throughout this work that the differences observed in inositol phosphate formation were not explained by or related to differences in the respective protein expression (*cf.* Figs. 1, *B* and *D*, 2, *D* and *F*, 3*D*, and 6*C* and Figs. S1–S6). All experiments were performed at least three times. Similar results and identical trends were obtained each time. Data from representative experiments are shown as mean values of triplicate determinations. In the experiments shown in Figs. 1*C*, 2, *A*–*C* and *E*, 3*C*, 4, and 6*A* and Table 1, background inositol phosphate formation in response to PLC and/or BTK expression was determined in parallel on cells transfected with empty vector and subtracted from the corresponding values, with appropriate consideration of error propagation for differences and quotients to determine the standard deviations of means (S.D.) of triplicate determinations (105). Although the S.D. values of these technical replicates are not shown in Figs. 1, *A*, *C*, and *E*, 2, *A*–*C*, *E*, and *G*, 3, *A*–*C*, 4, and 6, *A*, *B*, and *D*, and Table 1, their relationships to the corresponding means were calculated in aggregate for all mean values shown in these representations ($n = 500$) and found to be distributed with a median of 9.93%, with 95% confidence limits of 8.97% and 10.93%. In the experiments displayed in Figs. 1, *C* and *E*, 2, *C*, *E*, and *G*, 6, *B* and *D*, and 7, *B* and *C*, the data were fitted by nonlinear least-squares curve fitting using all replicate values to three- or four-parameter dose-response equations using GraphPad Prism®, version 4.03. In certain cases, the global curve–fitting procedure contained in Prism was used to determine whether the best-fit values of selected parameters differed between data sets. The simpler model was selected unless the extra sum of squares *F*-test had a *p* value of less than 0.05.

Data availability

All data are contained within the manuscript. Raw data as well as computer subroutines used for data processing and equations used to calculate propagation of experimental errors are available on request from Peter Gierschik (peter.gierschik@uni-ulm.de).

Author contributions—M. W., P. G., and C. W. conceptualization; M. W. and Y. I. H. validation; M. W., L. M., O. G., J. H., S. E., Y. Z., R. R., S. W., and C. W. investigation; M. W., O. G., Y. I. H., and C. W. visualization; M. W. methodology; S. S., E. H., Y. I. H., P. G., and C. W. writing-review and editing; Y. I. H. and P. G. writing-original draft; P. G. and C. W. data curation; P. G. and C. W. supervision; C. W. formal analysis.

Acknowledgments—We thank Pietro Taverna and Judy Fox from Sunesis Pharmaceuticals for critically reading the manuscript and for the gift of vecabrutinib. We thank the expert technical assistance of Norbert Zanker, Anita Ruepp, and Susanne Gierschik. The International Graduate School in Molecular Medicine, Ulm (IGradU), Germany, was funded within the Excellence Initiative of the German Federal and State Governments Grant GSC 279.

References

1. Koss, H., Bunney, T. D., Behjati, S., and Katan, M. (2014) Dysfunction of phospholipase Cγ in immune disorders and cancer. *Trends Biochem. Sci.* **39,** 603–611
2. Milner, J. D. (2015) PLAID: a syndrome of complex patterns of disease and unique phenotypes. *J. Clin. Immunol.* **35,** 527–530 CrossRef Medline
3. de Lange, K. M., Moutsianas, L., Lee, J. C., Lamb, C. A., Luo, Y., Kennedy, N. A., Jostins, L., Rice, D. L., Gutierrez-Achury, J., Ji, S.-G., Heap, G., Nimmo, E. R., Edwards, C., Henderson, P., Mowat, C., *et al.* (2017) Genome-wide association study implicates immune activation of multiple integrin genes in inflammatory bowel disease. *Nat. Genet.* **49,** 256–261 CrossRef Medline
4. Lane, B. M., Cason, R., Esezobor, C. I., and Gbadegesin, R. A. (2019) Genetics of childhood steroid sensitive nephrotic syndrome: an update. *Front. Pediatr.* **7,** 8 CrossRef Medline
5. Kogure, Y., and Kataoka, K. (2017) Genetic alterations in adult T-cell leukemia/lymphoma. *Cancer Sci.* **108,** 1719–1725 CrossRef Medline
6. Megquier, K., Turner-Maier, J., Swofford, R., Kim, J.-H., Sarver, A. L., Wang, C., Sakthikumar, S., Johnson, J., Koltookian, M., Lewellen, M., Scott, M. C., Schulte, A. J., Borst, L., Tonomura, N., Alfoldi, *et al.* (2019) Comparative genomics reveals shared mutational landscape in canine hemangiosarcoma and human angiosarcoma. *Mol. Cancer Res.* **17,** 2410–2421 CrossRef
7. Kaymaz, Y., Oduor, C. I., Yu, H., Otieno, J. A., Ong'echa, J. M., Moormann, A. M., and Bailey, J. A. (2017) Comprehensive transcriptome and mutational profiling of endemic Burkitt lymphoma reveals EBV type-specific differences. *Mol. Cancer Res.* **15,** 563–576 CrossRef Medline
8. Sasner, M., Williams, H. M., Oblak, A. L., O'Rourke, R., Preuss, C., Saykin, A. J., Rizzo, S. J. S., Ananda, G., Philip, V., Carter, G. W., Lamb, B. T., and Howell, G. (2018) Novel models of late-onset Alzheimer's disease based on GWAS. *Alzheimers Dement.* **14,** P1445 CrossRef
9. van der Lee, S. J., Conway, O. J., Jansen, I., Carrasquillo, M. M., Kleineidam, L., van den Akker, E., Hernández, I., van Eijk, K. R., Stringa, N., Chen, J. A., Zettergren, A., Andlauer, T. F. M., Diez-Fairen, M., Simon-Sanchez, J., Lleó, A., *et al.* (2019) A nonsynonymous mutation in PLCG2 reduces the risk of Alzheimer's disease, dementia with Lewy bodies and frontotemporal dementia, and increases the likelihood of longevity. *Acta Neuropathol.* **138,** 237–250 CrossRef Medline
10. Kaur, V., and Swami, A. (2017) Ibrutinib in CLL: a focus on adverse events, resistance, and novel approaches beyond ibrutinib. *Ann. Hematol.* **96,** 1175–1184 CrossRef Medline
11. Berg, L. J., Finkelstein, L. D., Lucas, J. A., and Schwartzberg, P. L. (2005) Tec family kinases in T lymphocyte development and function. *Annu. Rev. Immunol.* **23,** 549–600 CrossRef Medline
12. Andreotti, A. H., Joseph, R. E., Conley, J. M., Iwasa, J., and Berg, L. J. (2018) Multidomain control over Tec kinase activation state tunes the T cell response. *Annu. Rev. Immunol.* **36,** 549–578 CrossRef Medline
13. Takata, M., and Kurosaki, T. (1996) A role for Bruton's tyrosine kinase in B cell antigen receptor-mediated activation of phospholipase C-γ_2. *J. Exp. Med.* **184,** 31–40 CrossRef Medline
14. Watanabe, D., Hashimoto, S., Ishiai, M., Matsushita, M., Baba, Y., Kishimoto, T., Kurosaki, T., and Tsukada, S. (2001) Four tyrosine residues in phospholipase C-γ_2, identified as Btk-dependent phosphorylation sites, are required for B cell antigen receptor-coupled calcium signaling. *J. Biol. Chem.* **276,** 38595–38601 CrossRef Medline
15. Harden, T. K., and Sondek, J. (2006) Regulation of phospholipase C isozymes by ras superfamily GTPases. *Annu. Rev. Pharmacol. Toxicol.* **46,** 355–379 CrossRef Medline
16. Kadamur, G., and Ross, E. M. (2013) Mammalian phospholipase C. *Annu. Rev. Physiol.* **75,** 127–154 CrossRef Medline
17. Fu, C., Turck, C. W., Kurosaki, T., and Chan, A. C. (1998) BLNK: a central linker protein in B cell activation. *Immunity* **9,** 93–103 CrossRef Medline
18. Chiu, C. W., Dalton, M., Ishiai, M., Kurosaki, T., and Chan, A. C. (2002) BLNK: molecular scaffolding through 'cis'-mediated organization of signaling proteins. *EMBO J.* **21,** 6461–6472 CrossRef Medline
19. Li, T., Rawlings, D. J., Park, H., Kato, R. M., Witte, O. N., and Satterthwaite, A. B. (1997) Constitutive membrane association potentiates acti-

vation of Bruton tyrosine kinase. *Oncogene* **15,** 1375–1383 CrossRef Medline
20. Várnai, P., Rother, K. I., and Balla, T. (1999) Phosphatidylinositol 3-kinase–dependent membrane association of the Bruton's tyrosine kinase pleckstrin homology domain visualized in single living cells. *J. Biol. Chem.* **274,** 10983–10989 CrossRef Medline
21. Hubbard, S. R., and Till, J. H. (2000) Protein tyrosine kinase structure and function. *Annu. Rev. Biochem.* **69,** 373–398 CrossRef Medline
22. Márquez, J. A., Smith, C. I., Petoukhov, M. V., Lo Surdo, P., Mattsson, P. T., Knekt, M., Westlund, A., Scheffzek, K., Saraste, M., and Svergun, D. I. (2003) Conformation of full-length Bruton tyrosine kinase (Btk) from synchrotron X-ray solution scattering. *EMBO J.* **22,** 4616–4624 CrossRef Medline
23. Middendorp, S., Dingjan, G. M., Maas, A., Dahlenborg, K., and Hendriks, R. W. (2003) Function of Bruton's tyrosine kinase during B cell development is partially independent of its catalytic activity. *J. Immunol.* **171,** 5988–5996 CrossRef Medline
24. Middendorp, S., Zijlstra, A. J., Kersseboom, R., Dingjan, G. M., Jumaa, H., and Hendriks, R. W. (2005) Tumor suppressor function of Bruton tyrosine kinase is independent of its catalytic activity. *Blood* **105,** 259–265 CrossRef Medline
25. Saito, K., Tolias, K. F., Saci, A., Koon, H. B., Humphries, L. A., Scharenberg, A., Rawlings, D. J., Kinet, J.-P., and Carpenter, C. L. (2003) BTK regulates PtdIns-4,5-P_2 synthesis: importance for calcium signaling and PI3K activity. *Immunity* **19,** 669–678 CrossRef Medline
26. Hendriks, R. W., Yuvaraj, S., and Kil, L. P. (2014) Targeting Bruton's tyrosine kinase in B cell malignancies. *Nat. Rev. Cancer* **14,** 219–232 CrossRef Medline
27. Rogers, K. A., Mousa, L., Zhao, Q., Bhat, S. A., Byrd, J. C., El Boghdadly, Z., Guerrero, T., Levine, L. B., Lucas, F., Shindiapina, P., Sigmund, A. M., Sullivan, M., Wiczer, T. E., Woyach, J. A., and Awan, F. T. (2019) Incidence of opportunistic infections during ibrutinib treatment for B-cell malignancies. *Leukemia* **33,** 2527–2530 CrossRef Medline
28. Mato, A. R., Roeker, L. E., Allan, J. N., Pagel, J. M., Brander, D. M., Hill, B. T., Cheson, B. D., Furman, R. R., Lamanna, N., Tam, C. S., Handunnetti, S., Jacobs, R., Lansigan, F., Bhavsar, E., and Barr, P. M., *et al.* (2018) Outcomes of front-line ibrutinib treated CLL patients excluded from landmark clinical trial. *Am. J. Hematol* **93,** 1394–1401 CrossRef
29. Woyach, J. A., Ruppert, A. S., Heerema, N. A., Zhao, W., Booth, A. M., Ding, W., Bartlett, N. L., Brander, D. M., Barr, P. M., Rogers, K. A., Parikh, S. A., Coutre, S., Hurria, A., Brown, J. R., Lozanski, G., *et al.* (2018) Ibrutinib regimens versus chemoimmunotherapy in older patients with untreated CLL. *N. Engl. J. Med.* **379,** 2517–2528 CrossRef Medline
30. Berglöf, A., Hamasy, A., Meinke, S., Palma, M., Krstic, A., Månsson, R., Kimby, E., Österborg, A., and Smith, C. I. (2015) Targets for ibrutinib beyond B cell malignancies. *Scand. J. Immunol.* **82,** 208–217 CrossRef Medline
31. Ito, M., Shichita, T., Okada, M., Komine, R., Noguchi, Y., Yoshimura, A., and Morita, R. (2015) Bruton's tyrosine kinase is essential for NLRP3 inflammasome activation and contributes to ischaemic brain injury. *Nat. Commun.* **6,** 7360 CrossRef Medline
32. Molina-Cerrillo, J., Alonso-Gordoa, T., Gajate, P., and Grande, E. (2017) Bruton's tyrosine kinase (BTK) as a promising target in solid tumors. *Cancer Treat. Rev.* **58,** 41–50 CrossRef Medline
33. Lv, J., Wu, J., He, F., Qu, Y., Zhang, Q., and Yu, C. (2018) Development of Bruton's tyrosine kinase inhibitors for rheumatoid arthritis. *Curr. Med. Chem.* **25,** 5847–5859 CrossRef Medline
34. Maddocks, K. J., Ruppert, A. S., Lozanski, G., Heerema, N. A., Zhao, W., Abruzzo, L., Lozanski, A., Davis, M., Gordon, A., Smith, L. L., Mantel, R., Jones, J. A., Flynn, J. M., Jaglowski, S. M., Andritsos, L. A., *et al.* (2015) Etiology of ibrutinib therapy discontinuation and outcomes in patients with chronic lymphocytic leukemia. *JAMA Oncol.* **1,** 80–87 CrossRef Medline
35. Albitar, A., Ma, W., DeDios, I., Estella, J., Ahn, I., Farooqui, M., Wiestner, A., and Albitar, M. (2017) Using high-sensitivity sequencing for the detection of mutations in BTK and PLCγ2 genes in cellular and cell-free DNA and correlation with progression in patients treated with BTK inhibitors. *Oncotarget* **8,** 17936–17944 CrossRef Medline
36. Jones, D., Woyach, J. A., Zhao, W., Caruthers, S., Tu, H., Coleman, J., Byrd, J. C., Johnson, A. J., and Lozanski, G. (2017) PLCG2 C2 domain mutations co-occur with BTK and PLCG2 resistance mutations in chronic lymphocytic leukemia undergoing ibrutinib treatment. *Leukemia* **31,** 1645–1647 CrossRef Medline
37. Woyach, J. A., Ruppert, A. S., Guinn, D., Lehman, A., Blachly, J. S., Lozanski, A., Heerema, N. A., Zhao, W., Coleman, J., Jones, D., Abruzzo, L., Gordon, A., Mantel, R., Smith, L. L., McWhorter, S., *et al.* (2017) BTK^{C481S}-mediated resistance to ibrutinib in chronic lymphocytic leukemia. *J. Clin. Oncol.* **35,** 1437–1443 CrossRef Medline
38. Walliser, C., Hermkes, E., Schade, A., Wiese, S., Deinzer, J., Zapatka, M., Désiré, L., Mertens, D., Stilgenbauer, S., and Gierschik, P. (2016) The phospholipase C-γ_2 mutants R665W and L845F identified in ibrutinib-resistant chronic lymphocytic leukemia patients are hypersensitive to the Rho GTPase Rac2 protein. *J. Biol. Chem.* **291,** 22136–22148 CrossRef Medline
39. Walliser, C., Wist, M., Hermkes, E., Zhou, Y., Schade, A., Haas, J., Deinzer, J., Désiré, L., Li, S. S. C., Stilgenbauer, S., Milner, J. D., and Gierschik, P. (2018) Functional characterization of phospholipase C-γ_2 mutant protein causing both somatic ibrutinib resistance and a germline monogenic autoinflammatory disorder. *Oncotarget* **9,** 34357–34378 CrossRef Medline
40. Liu, T.-M., Woyach, J. A., Zhong, Y., Lozanski, A., Lozanski, G., Dong, S., Strattan, E., Lehman, A., Zhang, X., Jones, J. A., Flynn, J., Andritsos, L. A., Maddocks, K., Jaglowski, S. M., Blum, K. A., *et al.* (2015) Hypermorphic mutation of phospholipase C-γ2 acquired in ibrutinib-resistant CLL confers BTK independency upon B-cell receptor activation. *Blood* **126,** 61–68 CrossRef Medline
41. Brill, L. M., Salomon, A. R., Ficarro, S. B., Mukherji, M., Stettler-Gill, M., and Peters, E. C. (2004) Robust phosphoproteomic profiling of tyrosine phosphorylation sites from human T cells using immobilized metal affinity chromatography and tandem mass spectrometry. *Anal. Chem.* **76,** 2763–2772 CrossRef Medline
42. Rikova, K., Guo, A., Zeng, Q., Possemato, A., Yu, J., Haack, H., Nardone, J., Lee, K., Reeves, C., Li, Y., Hu, Y., Tan, Z., Stokes, M., Sullivan, L., Mitchell, J., *et al.* (2007) Global survey of phosphotyrosine signaling identifies oncogenic kinases in lung cancer. *Cell* **131,** 1190–1203 CrossRef Medline
43. Hicks, S. N., Jezyk, M. R., Gershburg, S., Seifert, J. P., Harden, T. K., and Sondek, J. (2008) General and versatile autoinhibition of PLC isozymes. *Mol. Cell* **31,** 383–394 CrossRef Medline
44. Bond, D. A., and Woyach, J. A. (2019) Targeting BTK in CLL: beyond ibrutinib. *Curr. Hematol. Malig. Rep.* **14,** 197–205 CrossRef Medline
45. Woyach, J. A., Furman, R. R., Liu, T.-M., Ozer, H. G., Zapatka, M., Ruppert, A. S., Xue, L., Li, D. H., Steggerda, S. M., Versele, M., Dave, S. S., Zhang, J., Yilmaz, A. S., Jaglowski, S. M., Blum, K. A., *et al.* (2014) Resistance mechanisms for the Bruton's tyrosine kinase inhibitor ibrutinib. *N. Engl. J. Med.* **370,** 2286–2294 CrossRef Medline
46. Burger, J. A., Landau, D. A., Taylor-Weiner, A., Bozic, I., Zhang, H., Sarosiek, K., Wang, L., Stewart, C., Fan, J., Hoellenriegel, J., Sivina, M., Dubuc, A. M., Fraser, C., Han, Y., Li, S., *et al.* (2016) Clonal evolution in patients with chronic lymphocytic leukemia developing resistance to BTK inhibition. *Nat. Commun.* **7,** 11589 CrossRef Medline
47. Berkovich, R., Wolfenson, H., Eisenberg, S., Ehrlich, M., Weiss, M., Klafter, J., Henis, Y. I., and Urbakh, M. (2011) Accurate quantification of diffusion and binding kinetics of non-integral membrane proteins by FRAP. *Traffic* **12,** 1648–1657 CrossRef Medline
48. Henis, Y. I., Rotblat, B., and Kloog, Y. (2006) FRAP beam-size analysis to measure palmitoylation-dependent membrane association dynamics and microdomain partitioning of Ras proteins. *Methods* **40,** 183–190 CrossRef Medline
49. Walliser, C., Tron, K., Clauss, K., Gutman, O., Kobitski, A. Y., Retlich, M., Schade, A., Röcker, C., Henis, Y. I., Nienhaus, G. U., and Gierschik, P. (2015) Rac-mediated stimulation of phospholipase Cγ_2 amplifies B-cell receptor-induced calcium signaling. *J. Biol. Chem.* **290,** 17056–17072 CrossRef Medline
50. Illenberger, D., Walliser, C., Strobel, J., Gutman, O., Niv, H., Gaidzik, V., Kloog, Y., Gierschik, P., and Henis, Y. I. (2003) Rac2 regulation of phos-

pholipase C-β_2 activity and mode of membrane interactions in intact cells. *J. Biol. Chem.* **278,** 8645–8652 CrossRef Medline
51. Fujiwara, T., Ritchie, K., Murakoshi, H., Jacobson, K., and Kusumi, A. (2002) Phospholipids undergo hop diffusion in compartmentalized cell membrane. *J. Cell Biol.* **157,** 1071–1081 CrossRef Medline
52. Ehrig, J., Petrov, E. P., and Schwille, P. (2011) Near-critical fluctuations and cytoskeleton-assisted phase separation lead to subdiffusion in cell membranes. *Biophys. J.* **100,** 80–89 CrossRef Medline
53. Walliser, C., Retlich, M., Harris, R., Everett, K. L., Josephs, M. B., Vatter, P., Esposito, D., Driscoll, P. C., Katan, M., Gierschik, P., and Bunney, T. D. (2008) Rac regulates its effector phospholipase Cγ_2 through interaction with a split pleckstrin homology domain. *J. Biol. Chem.* **283,** 30351–30362 CrossRef Medline
54. Bunney, T. D., Opaleye, O., Roe, S. M., Vatter, P., Baxendale, R. W., Walliser, C., Everett, K. L., Josephs, M. B., Christow, C., Rodrigues-Lima, F., Gierschik, P., Pearl, L. H., and Katan, M. (2009) Structural insights into formation of an active signaling complex between Rac and phospholipase Cγ_2. *Mol. Cell* **34,** 223–233 CrossRef Medline
55. Schade, A., Walliser, C., Wist, M., Haas, J., Vatter, P., Kraus, J. M., Filingeri, D., Havenith, G., Kestler, H. A., Milner, J. D., and Gierschik, P. (2016) Cool-temperature–mediated activation of phospholipase C-γ_2 in the human hereditary disease PLAID. *Cell. Signal.* **28,** 1237–1251 CrossRef Medline
56. Owen, C., Berinstein, N. L., Christofides, A., and Sehn, L. H. (2019) Review of Bruton tyrosine kinase inhibitors for the treatment of relapsed or refractory mantle cell lymphoma. *Curr. Oncol.* **26,** e233–e240 CrossRef Medline
57. Zhou, Q., Lee, G.-S., Brady, J., Datta, S., Katan, M., Sheikh, A., Martins, M. S., Bunney, T. D., Santich, B. H., Moir, S., Kuhns, D. B., Long Priel, D. A., Ombrello, A., Stone, D., Ombrello, M. J., *et al.* (2012) A hypermorphic missense mutation in PLCG2, encoding phospholipase Cγ_2, causes a dominantly inherited autoinflammatory disease with immunodeficiency. *Am. J. Hum. Genet.* **91,** 713–720 CrossRef Medline
58. Fluckiger, A.-C., Li, Z., Kato, R. M., Wahl, M. I., Ochs, H. D., Longnecker, R., Kinet, J.-P., Witte, O. N., Scharenberg, A. M., and Rawlings, D. J. (1998) Btk/Tec kinases regulate sustained increases in intracellular Ca^{2+} following B-cell receptor activation. *EMBO J.* **17,** 1973–1985 CrossRef Medline
59. Hashimoto, S., Iwamatsu, A., Ishiai, M., Okawa, K., Yamadori, T., Matsushita, M., Baba, Y., Kishimoto, T., Kurosaki, T., and Tsukada, S. (1999) Identification of the SH2 domain binding protein of Bruton's tyrosine kinase as BLNK—functional significance of Btk–SH2 domain in B-cell antigen receptor-coupled calcium signaling. *Blood* **94,** 2357–2364 CrossRef Medline
60. Rodriguez, R., Matsuda, M., Perisic, O., Bravo, J., Paul, A., Jones, N. P., Light, Y., Swann, K., Williams, R. L., and Katan, M. (2001) Tyrosine residues in phospholipase Cγ_2 essential for the enzyme function in B-cell signaling. *J. Biol. Chem.* **276,** 47982–47992 CrossRef Medline
61. Kurosaki, T., and Tsukada, S. (2000) BLNK: connecting Syk and Btk to calcium signals. *Immunity* **12,** 1–5 CrossRef Medline
62. Ishiai, M., Kurosaki, M., Pappu, R., Okawa, K., Ronko, I., Fu, C., Shibata, M., Iwamatsu, A., Chan, A. C., and Kurosaki, T. (1999) BLNK required for coupling Syk to PLCγ_2 and Rac1–JNK in B cells. *Immunity* **10,** 117–125 CrossRef Medline
63. Rodriguez, R., Matsuda, M., Storey, A., and Katan, M. (2003) Requirements for distinct steps of phospholipase Cγ_2 regulation, membrane-raft-dependent targeting and subsequent enzyme activation in B-cell signalling. *Biochem. J.* **374,** 269–280 CrossRef Medline
64. Udenwobele, D. I., Su, R.-C., Good, S. V., Ball, T. B., Varma Shrivastav, S., and Shrivastav, A. (2017) Myristoylation: an important protein modification in the immune response. *Front. Immunol.* **8,** 751 CrossRef Medline
65. Runft, L. L., Watras, J., and Jaffe, L. A. (1999) Calcium release at fertilization of *Xenopus* eggs requires type I IP_3 receptors, but not SH2 domain-mediated activation of PLCγ or G_q-mediated activation of PLCβ. *Dev. Biol.* **214,** 399–411 CrossRef Medline
66. Sato, K., Tokmakov, A. A., He, C.-L., Kurokawa, M., Iwasaki, T., Shirouzu, M., Fissore, R. A., Yokoyama, S., and Fukami, Y. (2003) Reconstitution of Src-dependent phospholipase Cγ phosphorylation and transient calcium release by using membrane rafts and cell-free extracts from *Xenopus* eggs. *J. Biol. Chem.* **278,** 38413–38420 CrossRef Medline
67. Cecchetti, S., Spadaro, F., Lugini, L., Podo, F., and Ramoni, C. (2007) Functional role of phosphatidylcholine-specific phospholipase C in regulating CD16 membrane expression in natural killer cells. *Eur. J. Immunol.* **37,** 2912–2922 CrossRef Medline
68. Kondadasula, S. V., Roda, J. M., Parihar, R., Yu, J., Lehman, A., Caligiuri, M. A., Tridandapani, S., Burry, R. W., and Carson, W. E., 3rd. (2008) Colocalization of the IL-12 receptor and FcγRIIIa to natural killer cell lipid rafts leads to activation of ERK and enhanced production of interferon-γ. *Blood* **111,** 4173–4183 CrossRef Medline
69. Aman, M. J., and Ravichandran, K. S. (2000) A requirement for lipid rafts in B-cell receptor induced Ca^{2+} flux. *Curr. Biol.* **10,** 393–396 CrossRef Medline
70. Guo, B., Kato, R. M., Garcia-Lloret, M., Wahl, M. I., and Rawlings, D. J. (2000) Engagement of the human pre-B-cell receptor generates a lipid raft-dependent calcium signaling complex. *Immunity* **13,** 243–253 CrossRef Medline
71. Pierce, S. K. (2002) Lipid rafts and B-cell activation. *Nat. Rev. Immunol.* **2,** 96–105 CrossRef Medline
72. Kroczek, C., Lang, C., Brachs, S., Grohmann, M., Dütting, S., Schweizer, A., Nitschke, L., Feller, S. M., Jäck, H.-M., and Mielenz, D. (2010) Swiprosin-1/EFhd2 controls B-cell receptor signaling through the assembly of the B-cell receptor, Syk, and phospholipase Cγ_2 in membrane rafts. *J. Immunol.* **184,** 3665–3676 CrossRef Medline
73. Phee, H., Rodgers, W., and Coggeshall, K. M. (2001) Visualization of negative signaling in B cells by quantitative confocal microscopy. *Mol. Cell. Biol.* **21,** 8615–8625 CrossRef Medline
74. Tomlinson, M. G., Woods, D. B., McMahon, M., Wahl, M. I., Witte, O. N., Kurosaki, T., Bolen, J. B., and Johnston, J. A. (2001) A conditional form of Bruton's tyrosine kinase is sufficient to activate multiple downstream signaling pathways via PLCγ_2 in B cells. *BMC Immunol.* **2,** 4 CrossRef Medline
75. Schwartzberg, P. L. (2003) Amplifying Btk's signal. *Immunity* **19,** 634–636 CrossRef Medline
76. Verí, M.-C., DeBell, K. E., Seminario, M.-C., DiBaldassarre, A., Reischl, I., Rawat, R., Graham, L., Noviello, C., Rellahan, B. L., Miscia, S., Wange, R. L., and Bonvini, E. (2001) Membrane raft-dependent regulation of phospholipase C-γ_1 activation in T lymphocytes. *Mol. Cell. Biol.* **21,** 6939–6950 CrossRef Medline
77. Clarke, C. J., Forman, S., Pritchett, J., Ohanian, V., and Ohanian, J. (2008) Phospholipase C-δ_1 modulates sustained contraction of rat mesenteric small arteries in response to noradrenaline, but not endothelin-1. *Am. J. Physiol. Heart Circ. Physiol.* **295,** H826–H834 CrossRef Medline
78. Stephenson, R. P. (1956) A modification of receptor theory. *Br. J. Pharmacol. Chemother.* **11,** 379–393
79. Waud, D. R. (1968) Pharmacological receptors. *Pharmacol. Rev.* **20,** 49–88 Medline
80. Butcher, R. W., Baird, C. E., and Sutherland, E. W. (1968) Effects of lipolytic and antilipolytic substances on adenosine 3′,5′-monophosphate levels in isolated fat cells. *J. Biol. Chem.* **243,** 1705–1712 Medline
81. Yamamura, H., and Rodbell, M. (1976) Hydroxybenzylpindolol and hydroxybenzylpropranolol: partial β-adrenergic agonists of adenylate cyclase in the rat adipocyte. *Mol. Pharmacol.* **12,** 693–700 Medline
82. Drummond, A. H., Baguley, B. C., and Staehelin, M. (1977) β-Adrenergic regulation of glycogen phosphorylase activity and adenosine cyclic 3′,5′-monophosphate accumulation in control and desensitized C-6 astrocytoma cells. *Mol. Pharmacol.* **13,** 1159–1169 Medline
83. Brooker, G. (1975) Implications of cyclic nucleotide oscillations during the myocardial contraction cycle. *Adv. Cyclic Nucleotide Res.* **5,** 435–452 Medline
84. Ramachandran, J. (1984) Corticotropin receptors, cyclic AMP and steroidogenesis. *Endocr. Res.* **10,** 347–363 CrossRef Medline
85. Prokocimer, P. G., Maze, M., Vickery, R. G., and Hoffman, B. B. (1988) Mechanism for desensitization of β-adrenergic receptor-stimulated lipolysis in adipocytes from rats harboring pheochromocytoma. *Endocrinology* **123,** 528–533 CrossRef Medline

86. Zhu, B. T. (1993) The competitive and noncompetitive antagonism of receptor-mediated drug actions in the presence of spare receptors. *J. Pharmacol. Toxicol. Methods* **29,** 85–91 CrossRef Medline
87. Ghia, P., Chiorazzi, N., and Stamatopoulos, K. (2008) Microenvironmental influences in chronic lymphocytic leukaemia: the role of antigen stimulation. *J. Intern. Med.* **264,** 549–562 CrossRef Medline
88. Stamatopoulos, K., Agathangelidis, A., Rosenquist, R., and Ghia, P. (2017) Antigen receptor stereotypy in chronic lymphocytic leukemia. *Leukemia* **31,** 282–291 CrossRef Medline
89. Dühren-von Minden, M., Übelhart, R., Schneider, D., Wossning, T., Bach, M. P., Buchner, M., Hofmann, D., Surova, E., Follo, M., Köhler, F., Wardemann, H., Zirlik, K., Veelken, H., and Jumaa, H. (2012) Chronic lymphocytic leukaemia is driven by antigen-independent cell-autonomous signalling. *Nature* **489,** 309–312 CrossRef Medline
90. Minici, C., Gounari, M., Übelhart, R., Scarfò, L., Dühren-von Minden, M., Schneider, D., Tasdogan, A., Alkhatib, A., Agathangelidis, A., Ntoufa, S., Chiorazzi, N., Jumaa, H., Stamatopoulos, K., Ghia, P., and Degano, M. (2017) Distinct homotypic B-cell receptor interactions shape the outcome of chronic lymphocytic leukaemia. *Nat. Commun.* **8,** 15746 CrossRef Medline
91. Ten Hacken, E., Gounari, M., Ghia, P., and Burger, J. A. (2019) The importance of B-cell receptor isotypes and stereotypes in chronic lymphocytic leukemia. *Leukemia* **33,** 287–298 CrossRef Medline
92. Conley, M. E., Fitch-Hilgenberg, M. E., Cleveland, J. L., Parolini, O., and Rohrer, J. (1994) Screening of genomic DNA to identify mutations in the gene for Bruton's tyrosine kinase. *Hum. Mol. Genet.* **3,** 1751–1756 CrossRef Medline
93. Kobayashi, S., Iwata, T., Saito, M., Iwasaki, R., Matsumoto, H., Naritaka, S., Kono, Y., and Hayashi, Y. (1996) Mutations of the Btk gene in 12 unrelated families with X-linked agammaglobulinemia in Japan. *Hum. Genet.* **97,** 424–430 CrossRef Medline
94. Carozzi, A. J., Kriz, R. W., Webster, C., and Parker, P. J. (1992) Identification, purification and characterization of a novel phosphatidylinositol-specific phospholipase C, a third member of the β-subfamily. *Eur. J. Biochem.* **210,** 521–529 CrossRef Medline
95. Struppe, J., Whiles, J. A., and Vold, R. R. (2000) Acidic phospholipid bicelles: a versatile model membrane system. *Biophys. J.* **78,** 281–289 CrossRef Medline
96. Piechulek, T., Rehlen, T., Walliser, C., Vatter, P., Moepps, B., and Gierschik, P. (2005) Isozyme-specific stimulation of phospholipase C-γ_2 by Rac GTPases. *J. Biol. Chem.* **280,** 38923–38931 CrossRef Medline
97. Gross, A., Kracher, B., Kraus, J. M., Kühlwein, S. D., Pfister, A. S., Wiese, S., Luckert, K., Pötz, O., Joos, T., Van Daele, D., De Raedt, L., Kühl, M., and Kestler, H. A. (2019) Representing dynamic biological networks with multi-scale probabilistic models. *Commun. Biol.* **2,** 21 CrossRef Medline
98. Fu, G., and Gascoigne, N. R. (2009) Multiplexed labeling of samples with cell tracking dyes facilitates rapid and accurate internally controlled calcium flux measurement by flow cytometry. *J. Immunol. Methods* **350,** 194–199 CrossRef Medline
99. Camps, M., Hou, C. F., Jakobs, K. H., and Gierschik, P. (1990) Guanosine 5′-[γ-thio]triphosphate-stimulated hydrolysis of phosphatidylinositol 4,5-bisphosphate in HL-60 granulocytes. Evidence that the guanine nucleotide acts by relieving phospholipase C from an inhibitory constraint. *Biochem. J.* **271,** 743–748 CrossRef Medline
100. Axelrod, D., Koppel, D. E., Schlessinger, J., Elson, E., and Webb, W. W. (1976) Mobility measurement by analysis of fluorescence photobleaching recovery kinetics. *Biophys. J.* **16,** 1055–1069 CrossRef Medline
101. Koppel, D. E., Axelrod, D., Schlessinger, J., Elson, E. L., and Webb, W. W. (1976) Dynamics of fluorescence marker concentration as a probe of mobility. *Biophys. J.* **16,** 1315–1329 CrossRef Medline
102. Petersen, T. (1986) Fitting parametric survival models with time-dependent covariates. *J. R. Stat. Soc. Ser. C Appl. Stat.* **35,** 281–288 CrossRef
103. Efron, B., and Tibshirani, R. J. (1994) The Bootstrap Estimate of Standard Error. In *An Introduction to the Bootstrap*, pp. 45–59, Chapman and Hall/CRC Press, Boca Raton, FL
104. Gutman, O., Walliser, C., Piechulek, T., Gierschik, P., and Henis, Y. I. (2010) Differential regulation of phospholipase C-β_2 activity and membrane interaction by Gαq, G$\beta_1\gamma_2$, and Rac2. *J. Biol. Chem.* **285,** 3905–3915 CrossRef Medline
105. Meyer, S. L. (1975) Propagation of Error and Least Squares. In *Data Analysis for Scientists and Engineers*, pp. 39–48, Peer Management Consultants, Evanston, IL